Collision kinematics in the western external Alps

Nicolas Bellahsen, Frédéric Mouthereau, Alexandre Boutoux, Mathieu Bellanger, Olivier Lacombe, Laurent Jolivet, Y. Rolland

AGU PUBLICATIONS

Tectonics

RESEARCH ARTICLE
10.1002/2013TC003453

Key Points:
- Five balanced cross sections of the western external Alps are presented
- Sequence of shortening and shortening and exhumation rates are determined
- The role of inherited Mesozoic margins on the collision kinematics is discussed

Correspondence to:
N. Bellahsen,
nicolas.bellahsen@upmc.fr

Citation:
Bellahsen, N., F. Mouthereau, A. Boutoux, M. Bellanger, O. Lacombe, L. Jolivet, and Y. Rolland (2014), Collision kinematics in the western external Alps, *Tectonics*, *33*, 1055–1088, doi:10.1002/2013TC003453.

Received 29 SEP 2013
Accepted 28 MAR 2014
Accepted article online 3 APR 2014
Published online 11 JUN 2014
Corrected 12 JUL 2014

This article was corrected on 12 JULY 2014. See the end of the full text for details.

Collision kinematics in the western external Alps

N. Bellahsen[1,2], F. Mouthereau[1,2], A. Boutoux[1,2], M. Bellanger[3,4], O. Lacombe[1,2], L. Jolivet[3], and Y. Rolland[5]

[1]Sorbonne Universités, UPMC Université Paris 06, UMR 7193, ISTeP, Paris, France, [2]CNRS, UMR 7193, ISTeP, Paris, France, [3]Université Orléans, ISTO, CNRS, UMR 7327, Orléans, France, [4]BRGM, DGR/GSO, Orléans, France, [5]Geoazur, UMR 7329, CNRS-UNS-UPMC-IRD, Valbonne, France

Abstract The kinematics of the collision in Western Alps are investigated through five balanced cross sections of the whole external domain from the Oisans to the Mont Blanc massif. These cross sections were built using published data for the Jura and subalpine fold-and-thrust belts and new structural and field analysis for the External Crystalline Massifs. Five units are defined: the sedimentary nappes from innermost parts of the external zone (e.g., ultra-Dauphinois/Helvetic), the crystalline units with their dysharmonically folded cover (e.g., Morcles nappe), sedimentary nappes over the frontal parts of the crystalline massifs (the Aravis-Granier unit), the subalpine belts (e.g., Vercors, Chartreuse, Bauges, and Bornes), and the Jura. Except for the ultra-Dauphinois nappes, the shortening, including the cover shortening, always corresponds to basement shortening. The total amount of shortening increases from south (28 km, 20%) to north (66 km, 27%). Moreover, the shortening is slightly older in the south than in the north; deepwater turbidites (flysch) and shallow marine to freshwater clastics (molasse) basins are more developed in the north; pressure and temperature conditions are higher in the north; the average uplift rates are about 3 times higher in the north and more localized in space. We propose that these differences are due to along-strike variations in the structure of the European continental margin inherited from Mesozoic times. We then build five palinspastic maps: one at Cretaceous times showing the inherited European Mesozoic margin structure and four from Priabonian to upper Miocene times showing the collision kinematics and the related rotation of Adria.

1. Introduction

Mountain belts and related collisional structures are often noncylindrical features. At the Alpine-Himalayan orogenic belt scale, for example, along-strike variations are observed in the timing, kinematics, and structural evolution during the Tethys closure and subsequent collision. These differences are not only due to variations in convergence velocities and finite shortening but may also reflect the inherited geometry of oceanic and rifted continental domains, and age-dependent rheological properties of the lithosphere [*Mouthereau et al.*, 2013], which may imply different subduction-collision dynamics.

At a smaller scale, within each segment of the whole Alpine-Himalayan belt, the differential precollisional history of rifted continental margins can therefore control the kinematics of the subsequent collision. Toward the lateral termination of an ocean, the structure may evolve from a fully oceanized basin, through an area where extension stopped after mantle exhumation, to an aborted rift. This is presently the case in the northern Red Sea [*Cochran and Martinez*, 1988] or in the Woodlark basin [*Taylor et al.*, 1995], for example. The along-strike variations of collision kinematics when such oceanic domains are closing and the role of the preorogenic extensional structures in the style and amount of shortening are still open questions.

The aim of this paper is to unravel the variations of tectonic evolution along strike of a mountain belt, in terms of shortening and associated exhumation rates as well as rheology and structural styles and to discuss the role of the preorogenic continental margins and rift structure. The Western Alps (Figure 1) are taken as a case study as it is one of the best known mountain belts by means of timing and tectonic evolution from subduction to collision stages. The overall history of subduction of the Ligurian ocean beneath Adria is now well known and documented: the subduction started during mid-Cretaceous times and ended during Paleogene times. However, *Handy et al.* [2010] (following *Stampfli et al.* [2002] and *Bousquet et al.* [2002, and references therein]) suggested that a Cretaceous Valais ocean opened between the proximal European margin and the distal Briançonnais domain, from the Eastern to the Western Alps. On the contrary, *Trumpy* [1975] and *Lemoine et al.* [1986] argued that it aborted westward in the present-day Western Alps. In the latter model, the opening of the Valais domain may have taken place during the Jurassic [*Manatschal et al.*, 2006; *Mohn et al.*, 2010; *Beltrando et al.*, 2012] or the Cretaceous

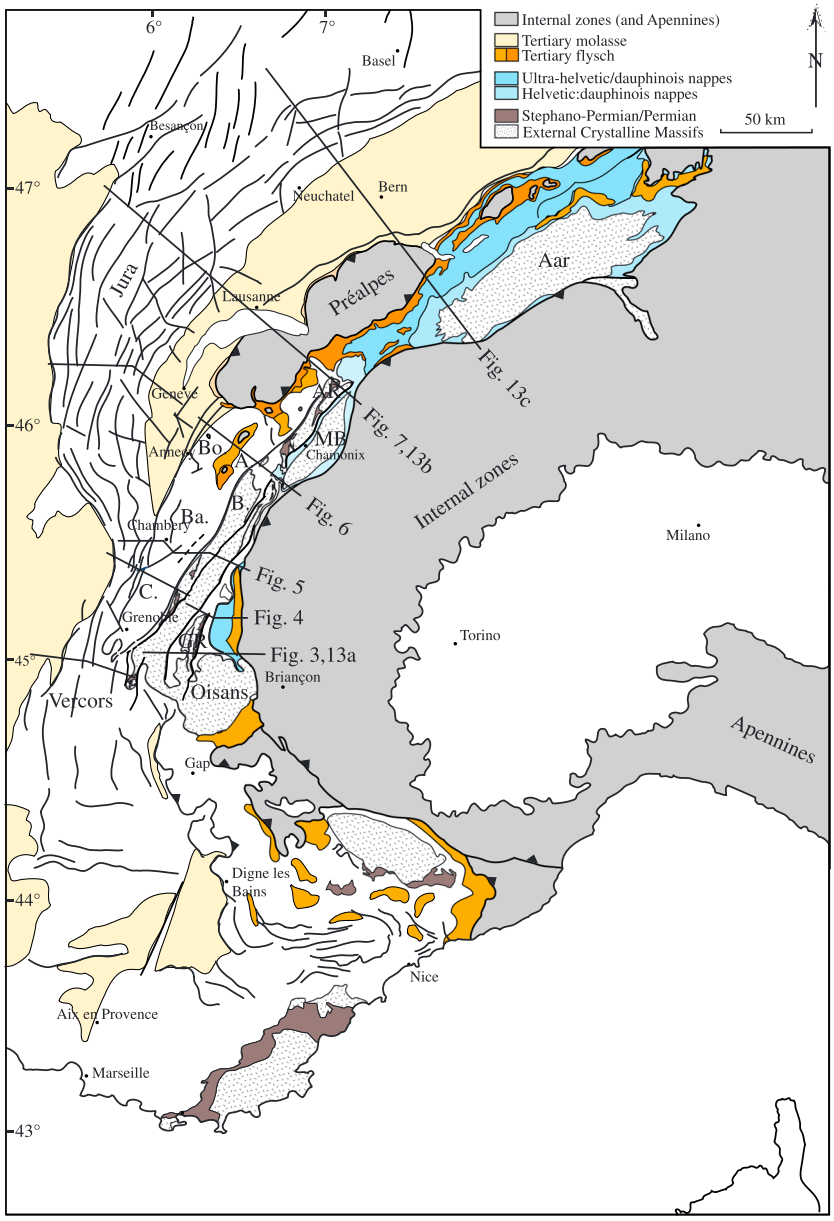

Figure 1. Structural map of the Western Alps. In gray are represented the internal units, including the Préalpes and the Sulens and Annes klippen (southwest of the Préalpes). Light blue areas are helvetic nappes (Morcles and Diablerets); darker blue areas represent the ultra-Helvetic and Ultra-Dauphinois nappes. Discontinuous straight lines give the locations of cross sections. Bo is for Bornes, AR for Aiguilles Rouges, MB for Mont Blanc, B for Belledonne, Ba for Bauges, C for Chartreuse, and GR for Grandes Rousses.

[*Loprieno et al.*, 2010]. The opening and closure of this domain is thus still debated but is an important issue as the different models imply different (thermal) structures of the European distal margins.

Within this framework and beyond the problem of the Mesozoic structure, many questions on the inversion of the Alpine margin are still pending. What is the true effect of the inherited normal faults? In analogue models of the Alpine collision [e.g., *Bonnet et al.*, 2007], the shortening of the underthrusted European crust is strongly controlled by the presence of weak inherited faults. This suggests that the crust was weakened because of inherited faults. However, there are no clear evidences in the field of the reactivation of such inherited faults and the weakening effect is mainly due to the soft synrift sedimentary rocks filling the fault-bounded basins [*Bellahsen et al.*, 2012] and fluid-rock interactions leading to the formation of phyllosilicates in shear zones with distinct orientations to the normal faults [e.g., *Wibberley*, 1999; *Bellanger et al.*, 2014].

Is the size (width and thickness) of the foreland basin linked to the growth of the orogenic load or rather to a slab pull effect? As noticed in *Bonnet et al.* [2007], the orogenic foreland basin grows in width and thickness until the basement units start to exhume. *Ford and Lickorish* [2004] showed that the northward transgression rate of the northern foreland basin strongly decreased in early Aquitanian times (around 23 Ma). This decrease occurred coevally with the onset of the exhumation in the External Crystalline Massifs (ECM, Figure 1, 22–23 Ma, Aar and Mont Blanc massifs [*Challandes et al.*, 2008; *Rolland et al.*, 2009]). On the other hand, the along-strike variations of the molassic basin, i.e., the decrease in both width and thickness from Central to Western Alps [e.g., *Ford et al.*, 2006], may be due to the western end of the orogenic load according to *Ford and Lickorish* [2004]. However, there was an orogenic load in Western Alps during Oligocene times (in the western ECM [*Dumont et al.*, 2008; *Bellahsen et al.*, 2012; *Bellanger et al.*, 2014]). Thus, the role of the orogenic load is still poorly understood.

To answer these questions, a prerequisite is a robust data set of finite shortening estimates over the whole Western Alps. Amounts of shortening seem to increase from the Western and Southwestern Alps toward the Central Alps [e.g., *Sinclair*, 1997; *Ford and Lickorish*, 2004; *Kempf and Pfiffner*, 2004], although there is to date no systematic and quantitative analysis of the rates all along the Western Alpine arc. Thus, we do not have clear quantification of the evolution of the Alpine wedge deformation toward its lateral western termination.

A reappraisal of shortening estimated over the whole Western Alps is proposed here and synthesized in the new data set. This data set is based on five balanced cross sections of the whole external zone from the Oisans to the Mont Blanc massifs. Structural style and sequence of shortening are documented and found to be consistent at the scale of the whole Western Alpine external arc. The amount of shortening for each deformation phase is discussed in the light of the timing and rate of cooling defined in the External Crystalline Massifs (ECMs) from a synthesis of published low-temperature thermochronology and pressure, temperature, time (P,T,t) constraints. Finally, palinspastic maps are presented for various Tertiary times and Middle Cretaceous times to discuss both the collision kinematics and the role of the inherited Mesozoic margin structure.

2. Geological Setting of Western Alps

The Alps are the result of the closure of the Ligurian ocean. In the Western Alps (Figure 1), Ligurian oceanic subduction started during Cretaceous times and lasted until late Paleocene to early Eocene times. Indeed, at that time, the first high pressure/low temperature (HP/LT) event is recorded in oceanic units before their exhumation [e.g., *Agard et al.*, 2002, and references therein]. Continental subduction is recorded as middle to upper Eocene, with the HP to Ultra-High Pressure (UHP) metamorphism of the alpine internal crystalline massifs (e.g., Dora Maira [*Duchene et al.*, 1997; *Rubatto and Hermann*, 2001; *Oberhänsli et al.*, 2004]) and the HP metamorphism of the Briançonnais unit (e.g., Vanoise [*Oberhänsli et al.*, 2004]). Collisional crustal thickening and orogenic development started during Oligocene times (Figure 2) with shortening of the external Alps and associated burial/exhumation (Dauphinois in France and Helvetic in Switzerland), especially the External Crystalline Massifs (ECM). In the following, we present a synthesis of the main studies on the external zone.

2.1. The External Crystalline Massifs and Their Sedimentary Nappes: Timing of Alpine Metamorphism, Shortening, and P,T Conditions

The Alpine ECM are composed from south to north of the following: the Argentera-Mercantour in the southwestern Alps; the Oisans, Grandes Rousses, Belledonne, Mont Blanc, and Aiguilles Rouges massifs in the Western Alps; and the Aar and Gothard massifs in the central Alps.

In the Argentera-Mercantour massif, two main NW-SE dextral transpressive shear zones were active between 34 and 20 Ma, according to $^{40}Ar/^{39}Ar$ on synkinematic phengites, at about 375°C and 5–7 kb [*Sanchez et al.*, 2011]. E-W reverse shear zones were active around 22–23 Ma [*Corsini et al.*, 2004] or range between 20 and 26 Ma [*Sanchez et al.*, 2011], which witness a N-S shortening that has continued since then [*Bauve et al.*, 2014].

In the Oisans massif (Figure 3), the main shortening phase is E-W [*Dumont et al.*, 2008, 2011, 2012; *Bellahsen et al.*, 2012; *Boutoux et al.*, 2014; *Bellanger et al.*, 2014], although there was oblique shortening at certain times and in certain places [*Dumont et al.*, 2008; *Bellanger et al.*, 2014]. *Simon-Labric et al.* [2009] showed that the earliest E-W alpine shortening (witnessed by strike-slip shear zones) started around 34–31 Ma. In the southern part of the massif, an Eocene N-S shortening phase has been recognized, which is sealed by the deposition of late Eocene sediments. At the Eocene-Oligocene boundary, a N-S to NW-SE shortening phase is identified: while *Dumont et al.* [2008] proposed that it affected the entire western ECM, *Bellanger et al.* [2014] showed

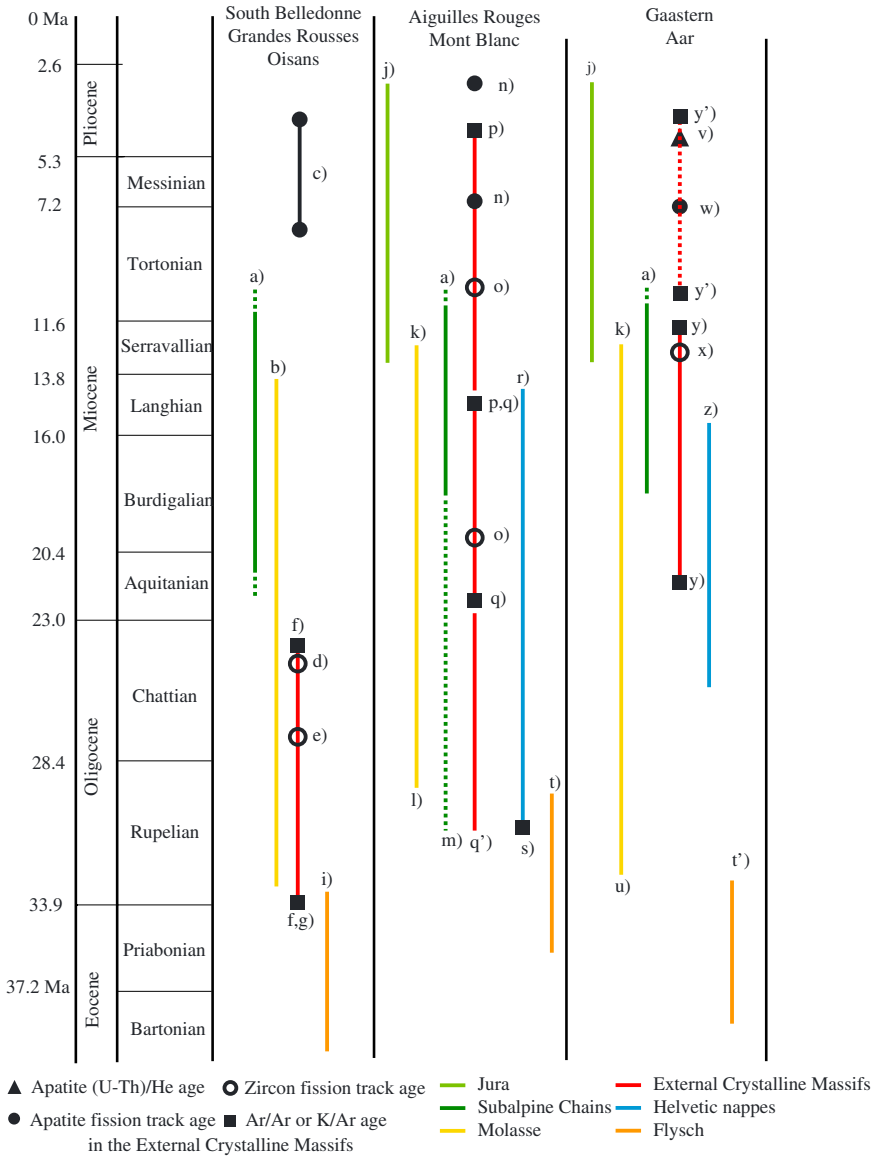

Figure 2. Synthesis of tectonic and sedimentary events in the western external Alps. Color bars are for the age of formation or deformation of the following units. For error bars and details on ages, see the cited references below. South Belledone/Grandes Rousses/Oisans: (a) Main phase of folding in the subalpine chains (Vercors, Chartreuse, Bauges) after *Arnaud* [1975]. (b) Age of shallow marine to freshwater clastics deposit [see *Ford and Lickorish*, 2004; *Ford et al.*, 2006]. (c) AFT age range in Grandes Rousses and Oisans [see *Vernon et al.*, 2008]. (d) Minimal age of the Grandes Rousses exhumation from thermopaleomagnitism [*Crouzet et al.*, 2001]. (e) Minimal age of the Oisans massif (La Meije) exhumation onset from thermochronology in *van der Beek et al.* [2010]. (f) Age of the Oisans massif shortening from $^{40}Ar/^{39}Ar$ data (M. Bellanger et al., The shortening of the European Dauphinois margin (Ecrins-Pelvoux Massif, Western Alps): New insights from T estimates and in-situ 40Ar/39Ar ages from basement reverse shear zones, submitted to *Journal of Geodynamics*, 2014). (g) Age of the eastern Oisans massif shortening [*Simon-Labric et al.*, 2009]. (i) End of the turbiditic sequence, "schistes à blocs" [*Kerckhove*, 1969; *Fry*, 1989; *Mulder et al.*, 2010]. Aiguilles Rouges/Mont Blanc: (j) Main Jura folding phase [*Bolliger et al.*, 1993; *Steiniger et al.*, 1996; *Kalin*, 1997; *Becker*, 2000]. (k) End of overfilled basin [*Ford et al.*, 2006]. (l) Onset of overfilled basin and (t) end of underfilled basin [*Sinclair*, 1997]. (m) Onset of subalpine chains shortening [*Leloup et al.*, 2005]. (n) AFT ages [*Carpena*, 1992; *Seward and Mancktelow*, 1994; *Leloup et al.*, 2005]. (o) ZFT ages [*Soom*, 1990; *Seward and Mancktelow*, 1994; *Leloup et al.*, 2005]. (p and q) Onset and end of Mont Blanc shear zones from $^{40}Ar/^{39}Ar$ [*Leloup et al.*, 2005; *Rolland et al.*, 2008], respectively. (q') Onset of Mont Blanc deformation [*Cenki-Tok et al.*, 2013]. (r) End of helvetic nappes deformation (Morcles) [*Kirschner et al.*, 1996] and (s) their onset [*Huon et al.*, 1994; *Crespo-Blanc et al.*, 1995]. (t and t') End of underfilled basin [*Sinclair*, 1997]. Gaastern/Aar/Gothard: (u) Onset of overfilled basin [*Sinclair*, 1997]. (v) UTh/He age [*Reinecker et al.*, 2008]. (w) AFT data [*Reinecker et al.*, 2008]. (x) ZFT data [*Michalski and Soom*, 1990]. (y) Age of shortening from $^{40}Ar/^{39}Ar$ in shear zones [*Challandes et al.*, 2008; *Rolland et al.*, 2009]. (y') Age of brittle faults in the Aar massif [*Kralik et al.*, 1992; *Hofmann et al.*, 2004].

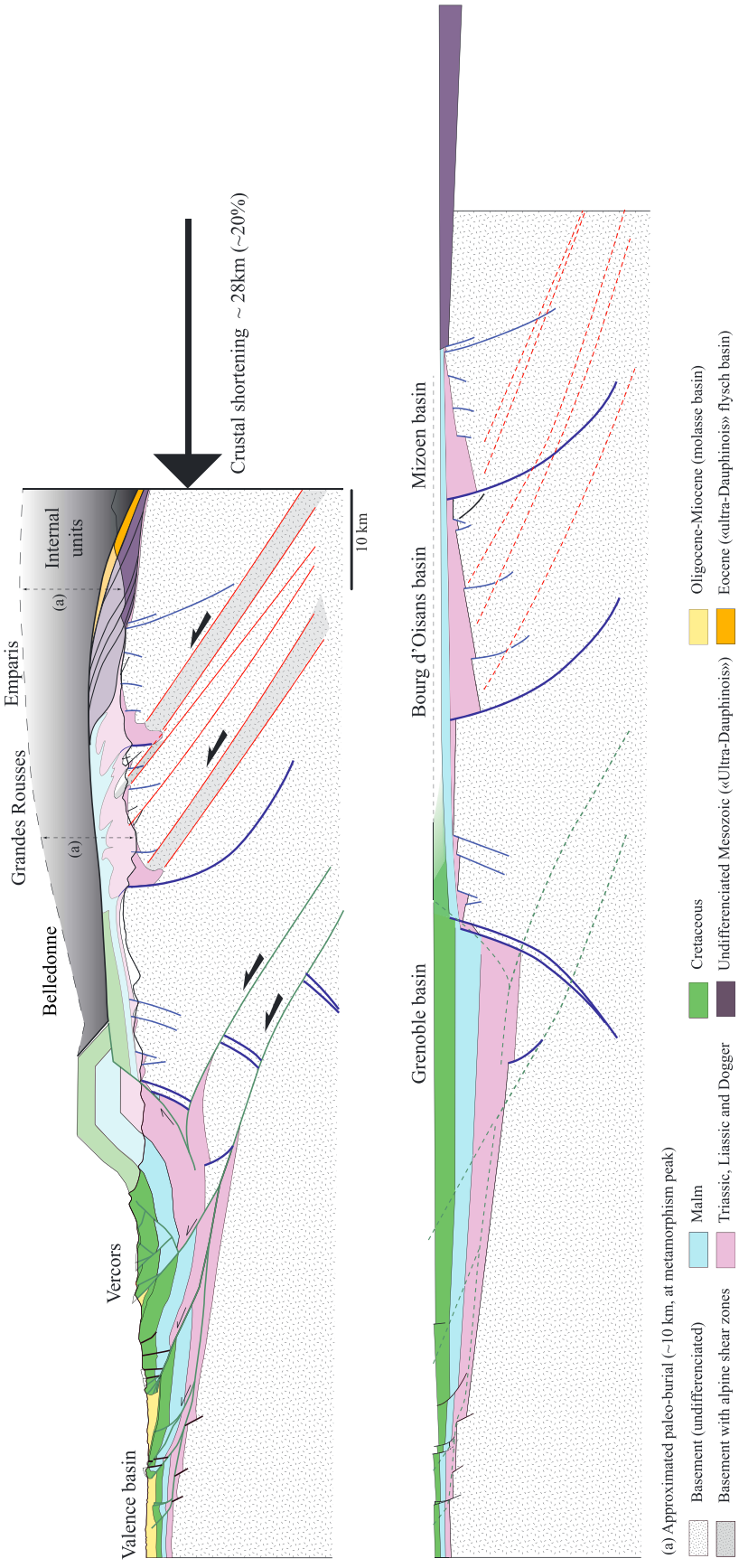

Figure 3. Balanced cross section through the Vercors-Oisans-Grandes Rousses-south Belledonne massifs: the Vercors-Oisans cross section [*Bellahsen et al.*, 2012], the subalpine part (Vercors) being redrawn from *Deville et al.* [1994] and constrained by seismic data. An amount of shortening 28 km is recorded for the whole external zone: 11.5 km for the ECM during Oligocene-early Miocene times characterized by large basement Alpine shear zones above which the cover is disharmonically folded, 16.5 km for the subalpine chain whose thrusts root in a décollement within Liassic layers activated by frontal basement thrusts beneath the ECM. The inherited Liassic basins localized the Alpine shortening, although their bounding normal faults were not reactivated. In dark purple are represented detached Mesozoic (mainly Jurassic, ultra-Dauphinois) layers that were not taken into account in the crustal restoration of the Alpine shortening. They most probably witness a (early?) stage of thin-skinned tectonics. See text for explanation and discussion.

that it may be restricted to the cover in a narrow zone below the Penninic Frontal Thrust. This latter observation is consistent with field evidences further north [*Ceriani and Schmid*, 2004].

The ECM at the Oisans latitude can be divided into several units from west to east: the south Belledonne, Grandes Rousses, and Emparis units (Figure 3). Further southeast, two other units are present: the Meije and Combeynot units [*Bellanger et al.*, 2014, and references therein]. The total amount of shortening at this latitude is about 28 km, including 11.5 km accommodated within the ECM [*Bellahsen et al.*, 2012], where the sedimentary cover is not significantly detached over the basement but is rather disharmonically deformed over it. Dysharmony or folds tightening in the cover is particularly well expressed above basement shear zones, displaying clear west verging kinematics. In the basement, the Alpine schistosity appears to be parallel to the inherited Variscan foliation, while the Alpine shear zones clearly deformed it. The shortening of these units occurred under green schist facies conditions (3–4 kb and 300–350°C) [*Jullien and Goffé*, 1993; *Simon-Labric et al.*, 2009]. The exhumation of these units started at least at 27 Ma from zircon fission track thermochronology (ZFT age) [*van der Beek et al.*, 2010] for the Meije massif (NE Oisans) and at least at 24 Ma from thermopaleomagnetism [*Crouzet et al.*, 2001] for the Grandes Rousses massif. Apatite fission track (AFT) showed that these massifs cooled through the 110°C isotherm at about 3–8 Ma (see a synthesis in *Vernon et al.* [2008]).

In the northern Belledonne massif, only few data are available. *Marquer et al.* [2006] described steep anastomosed brittle-ductile shear zones developed under green schist conditions. This Alpine kinematics is compatible with a NW-SE shortening along with a strong vertical stretching.

In the Mont Blanc massif (Figure 1), the development of anastomosed steep shear zones with a flower-type structure combining top-to-NW and SE sense of shear, along with right-lateral movements, mainly ranges from 22 to 15 Ma ($^{40}Ar/^{39}Ar$ on phengites [*Rolland et al.*, 2008]) at around 400°C and 5 kb [*Rolland et al.*, 2003]. Recently, ages of 29 ± 1 Ma were obtained from in situ allanite U-Pb dating in central Mont Blanc shear zones [*Cenki-Tok et al.*, 2013], which suggests that the onset of the shortening could be older (Figure 2).

In the Aiguilles Rouges massif, few ages of deformation are available in the literature. *Leloup et al.* [2005] considered that the uplift started around 20 Ma, which is consistent with the structural interpretation of *Burkhard and Sommaruga* [1998] where the upper Aiguilles Rouges basement thrusts were active during the OSM (Upper Freshwater Molasse) deposition, i.e., since 16 Ma. In both the Mont Blanc and the Aiguilles Rouges massifs, ZFT ages are about 8–15 Ma even though some data show older ages up to more than 20 Ma (Figure 2); AFT ages are about 3–8 Ma [*Vernon et al.*, 2008]. Similar ages are found for the Belledonne massif, although scarcer.

In the Aar massif, the main shearing event (along NE-SW shear zones) occurred between 17 and 21 Ma at 400–450°C and 6 kb [*Challandes et al.*, 2008] or 20–22 Ma [*Rolland et al.*, 2009] with west verging kinematics and was followed by reverse to dextral shear zones at 12–14 Ma [*Rolland et al.*, 2009]. Finally, brittle deformations have occurred since 9–5 Ma [*Kralik et al.*, 1992] and probably until 3 Ma [*Hofmann et al.*, 2004] (Figure 2). The kinematics of shortening during the first phase corresponds to a NW-SE contraction marked in the field by anastomozed shear zones, rather steep in the internal parts and/or even east verging (Gothard massif) [*Marquer*, 1990], while they are west verging in the more frontal parts [*Burkhard*, 1988]. The shortening is most likely younger in the Gaastern massif and older in the Gothard massif [*Burkhard*, 1988].

In the external Alps, large units structurally above the ECM known as sedimentary nappes have been described: the Morcles, Diablerets, Wildhorn, and Doldenhorn nappes [e.g., *Ramsay*, 1981]. The Morcles and Doldenhorn nappes ("Helvetic nappes," Figure 1) are the cover of the Mont Blanc and the Aar massifs, respectively [*Escher et al.*, 1993; *Burkhard*, 1988; *Ramsay*, 1981], or less probably of subducted crust now buried below the internal units southeast of the Mont Blanc massif [*Leloup et al.*, 2005]. The Diablerets and the Wildhorn nappes ("ultra-Helvetic nappes," Figure 1) are associated to the innermost part of the external zone, in the east or southeast [e.g., *Ramsay*, 1981; *Burkhard and Sommaruga*, 1998]. They are made of Mesozoic and Cenozoic sedimentary rocks: Triassic, Jurassic, and Cretaceous layers are quite thick (especially in the Wildhorn nappe) and are overlain by ultra-helvetic deepwater turbidites (Eocene flysch). These units are structurally located below the penninic units and are the oldest units of the external zone. They were emplaced along a NW-SE direction [*Ramsay*, 1981] with a thin-skinned structural style [*Burkhard and Sommaruga*, 1998].

2.2. The External Fold-and-Thrust Belt and Foreland Basin Evolution

From south to north, the fold-and-thrust belts are named as follows: Vercors, Chartreuse, Bauges, Bornes-Aravis, and Chablais-Haut Giffre, as well as the Jura. Except for the latter, the age of shortening is usually

considered as being middle Miocene (Figure 2), the Burdigalian-Langhian shallow marine clastics being syntectonic in the Vercors massif [*Arnaud*, 1975] and the middle Miocene shallow marine clastics being syntectonic north of the Prealpes [see *Burkhard and Sommaruga*, 1998, and references therein]. The subalpine chains are composed of Mesozoic and Cenozoic sedimentary rocks. While the Mesozoic rocks are mainly carbonate, the Cenozoic ones are mainly siliciclastic: Oligocene and/or Miocene shallow marine to freshwater clastics (and carbonates) can be found, and these molassic series witness the uplift and erosion of more internal areas. In these massifs, the thrusts root in a décollement layer located within the (upper Triassic-) Liassic series [*Deville et al.*, 1994; *Philippe et al.*, 1998; *Affolter et al.*, 2008].

The Jura fold-and-thrust belt shortening occurred from Serravallian times to Early Pliocene times (Figure 2) [*Bolliger et al.*, 1993; *Steiniger et al.*, 1996; *Kalin*, 1997; *Becker*, 2000]. Unlike the Vercors massif, the décollement level is located within the Triassic evaporites. Within these belts, the shortening directions are quite consistent, roughly perpendicular to the alpine arc: from WNW-ESE in the Vercors-Chartreuse [*Philippe et al.*, 1998] to globally NW-SE in Jura (subperpendicular to the main folds and thrusts) even if two successive directions are observed in southern Jura and linked to the arc evolution [*Homberg et al.*, 1999].

The position of the footwall cutoff is still a matter of debate. The décollement at the cover base may root in basement thrust ramps below the ECM or may be instead folded above the ECM, rooting eastward. There are evidences that the former occurred, especially based on seismic data [*Pfiffner et al.*, 1997; *Steck et al.*, 1997; *Deville and Chauvière*, 2000]. This is detailed further down.

In southern Oisans, Tertiary sedimentary rocks directly overlie the basement. They are Priabonian in age (and lowermost Oligocene for the formation top) and composed of three typical facies: shallow water limestones, pelagic marls, and deepwater turbidites. This trinity represents the sedimentation in the underfilled subsiding foreland basin [*Sinclair*, 1997] whose turbiditic succession is regionally referred to as the flysch facies. In northern Oisans, similar series ("Aiguilles d'Arves flysch") are overthrusted over the Mesozoic cover, and their age is similar to the southern Oisans one. Their initial paleogeographical position is, however, more difficult to define. Around the Mont Blanc/Aiguilles Rouges massifs, the underfilled trinity is younger, the whole turbidites series being Oligocene (up to Rupelian, around 30 Ma), while it is slightly older in the Aar massif area (up to early Rupelian, around 34 Ma) [*Sinclair*, 1997]. The deepening upward stratigraphy of these Eocene-Oligocene series was mapped out all around the Alpine arc [*Sinclair*, 1997] and was modeled as a migrating flexural basin [*Ford et al.*, 1999].

The molasse basin is an overfilled basin [*Sinclair and Allen*, 1992] with both shallow marine to freshwater clastics. In the Western Alps, the Oligocene freshwater clastic series are rather thin and restricted to small basins [*Ford et al.*, 2006], the main depocenters being localized in the Devoluy (west of Gap, Figure 1) or in the Barrême syncline for example, while the Miocene shallow marine clastics are more widespread but also rather thin. In the North Alpine Foreland Basin (NAFB), in the western central Alps, the shallow marine to freshwater clastic series (molasse) are very thick (up to 4 km [*Burkhard and Sommaruga*, 1998] and possibly even more [*Bonnet et al.*, 2007]). The zone of transition between these two subbasins (thin in the west and thick further northeast) is located around Chambéry in Savoie (Figure 1) [*Ford and Lickorish*, 2004]. Thus, there was no large molassic basin in SE France, while in the north the overfilled flexural basin migrated northward at the same rate as the underfilled one (around 10 mm yr^{-1} [*Ford et al.*, 2006]) until Aquitanian times and then slowed down [*Sinclair*, 1997].

2.3. Open Questions on Structural Styles

There is a large consensus on the fact that the ECM are allochthonous: geophysical data show that the subalpine chains were deformed above a basal sedimentary décollement kinematically linked to frontal basement thrust ramps [*Deville et al.*, 1994; *Pfiffner et al.*, 1997; *Burkhard and Sommaruga*, 1998; *Deville and Chauvière*, 2000], connecting downdip to a middle lower crustal detachment. In such a perspective, the propagation of the deformation in the outermost part of the fold-and-thrust belt, i.e., the Jura, is necessarily also linked to the presence of basement thrusts below the ECM and not associated eastward to a décollement at the cover base above the ECMs: once the ECM started to be uplifted, it is likely that a décollement at the basement-cover interface of ECM would be unactivated. This is consistent with $^{40}Ar/^{39}Ar$ ages in *Rolland et al.* [2008] and *Cenki-Tok et al.* [2013] that clearly indicate that the Mont Blanc massif started to shorten before the Jura shortening.

Less clear, however, is the structural style of the inner part of the fold-and-thrust belt. In the north, it appears that the Morcles nappe is the Mont Blanc cover [*Escher et al.*, 1993; *Burkhard and Sommaruga*, 1998]; in the northeastern Aiguilles Rouges massifs, the subalpine chain is very limited and most of the equivalent shortening is accommodated in the molassic series (shallow marine to freshwater clastics, NAFB) between the Préalpes and the Jura [*Burkhard and Sommaruga*, 1998]. Thus, the Mont Blanc cover is not strongly detached and transported toward the NW. Similarly, further south, the cover of the Oisans massif is not detached above its basement but is rather disharmonically folded above basement shear zones [*Bellahsen et al.*, 2012]. Thus, northeast of the Mont Blanc massif and in the Oisans Massif, the subalpine belts cannot be the former cover of the ECM as previously proposed by *Doudoux et al.* [1982].

According to these authors, the Bauges and the Bornes massifs are equivalent to the Morcles nappe. Thus, they would represent the cover of the internal Belledonne and the Mont Blanc massifs. *Leloup et al.* [2005] even assumed that the Bauges and Bornes massifs are the cover of units located southeast of the Mont Blanc massif. However, further south, it is clear that the Chartreuse and Vercors massifs are not the cover of the Belledonne basement, or at best it is the cover of its outermost part in some places [*Deville et al.*, 1994; *Deville and Chauvière*, 2000; *Philippe et al.*, 1998; *Bellahsen et al.*, 2012].

Alternatively, *Epard* [1990] proposed that the Mont Joly unit (SW Mont Blanc, Figure 1) is the equivalent of the Morcles nappe. Indeed, it represents the former cover of the southwestern termination of the Mont Blanc massif. This unit is only composed of the Triassic and Liassic layers. It remains unclear whether the upper part of the cover was detached from the lower part or not: northwest of the Mont Joly, the Mesozoic series of the Aravis massif may represent layers slightly detached from the Mont Joly unit.

To address these questions, we present regional cross sections assuming that all (or part) of both the subalpine chains and the Jura shortening are linked to basement thrusts beneath the ECMs [*Burkhard and Sommaruga*, 1998; *Deville and Chauvière*, 2000]. The cross sections aim at defining the structural styles for the whole external zone as well as the sequence of deformation and at providing rates of both shortening and exhumation. The along-strike structural variations are finally tentatively interpreted in terms of preorogenic geometry of the European passive margin.

3. Regional Balanced Cross Sections

In this part, we present five cross sections (Figures 3–7): two from the literature, the Vercors-Oisans section [*Bellahsen et al.*, 2012] and the Prealpes-Mont Blanc section [*Burkhard and Sommaruga*, 1998]; and three new ones, the Chartreuse-Grandes Rousses, Chartreuse-Belledonne, and Bornes-Mont Blanc cross sections. These three new cross sections have been balanced using assumptions detailed in *Bellahsen et al.* [2012]. These main assumptions are, for the ECM part of the section, constant surface for the sedimentary cover and constant length for the basement top (determined from the lower Triassic layers still attached to the basement and either mapped in the field or redrawn from geological maps). The outermost part of the sections (i.e., the fold-and-thrust belts) have been redrawn from the literature and constrained by seismic data; constant length and area were considered for the restoration [*Deville et al.*, 1994; *Philippe et al.*, 1998; *Affolter et al.*, 2008].

3.1. The Vercors-Oisans Cross Section

This cross section (Figure 3) has been published in *Bellahsen et al.* [2012]. Thus, here we will only sum up the main insights. Several alpine shear zones deformed the basement in the Oisans, Grandes Rousses, and south Belledonne basement, most probably during Oligocene times, as the shortening later localized west of these shear zones on the frontal ramps during Miocene times. Such shear zones account for an amount of shortening of 11.5 km, while the frontal ramps below south Belledonne massif account for 16.5 km.

The ultra-Dauphinois flysch unit (deepwater turbidites) to the east is allochthonous. *Bellanger et al.* [2014] showed that it underwent NW-SE shortening. Thus, it must be restored somewhere east or southeast of the section (see further down). In any case, it shows that the alpine crustal shortening in the Oisans massif occurred west or northwest of the turbiditic basin.

In the ECM, the inherited Liassic normal faults were not reactivated [*Bellahsen et al.*, 2012]. Three main inherited normal faults were recognized: the faults controlling the Grenoble, Bourg d'Oisans, and Mizoen basins (Figure 3), the former being the deepest as attested by the very thick Mesozoic sedimentary

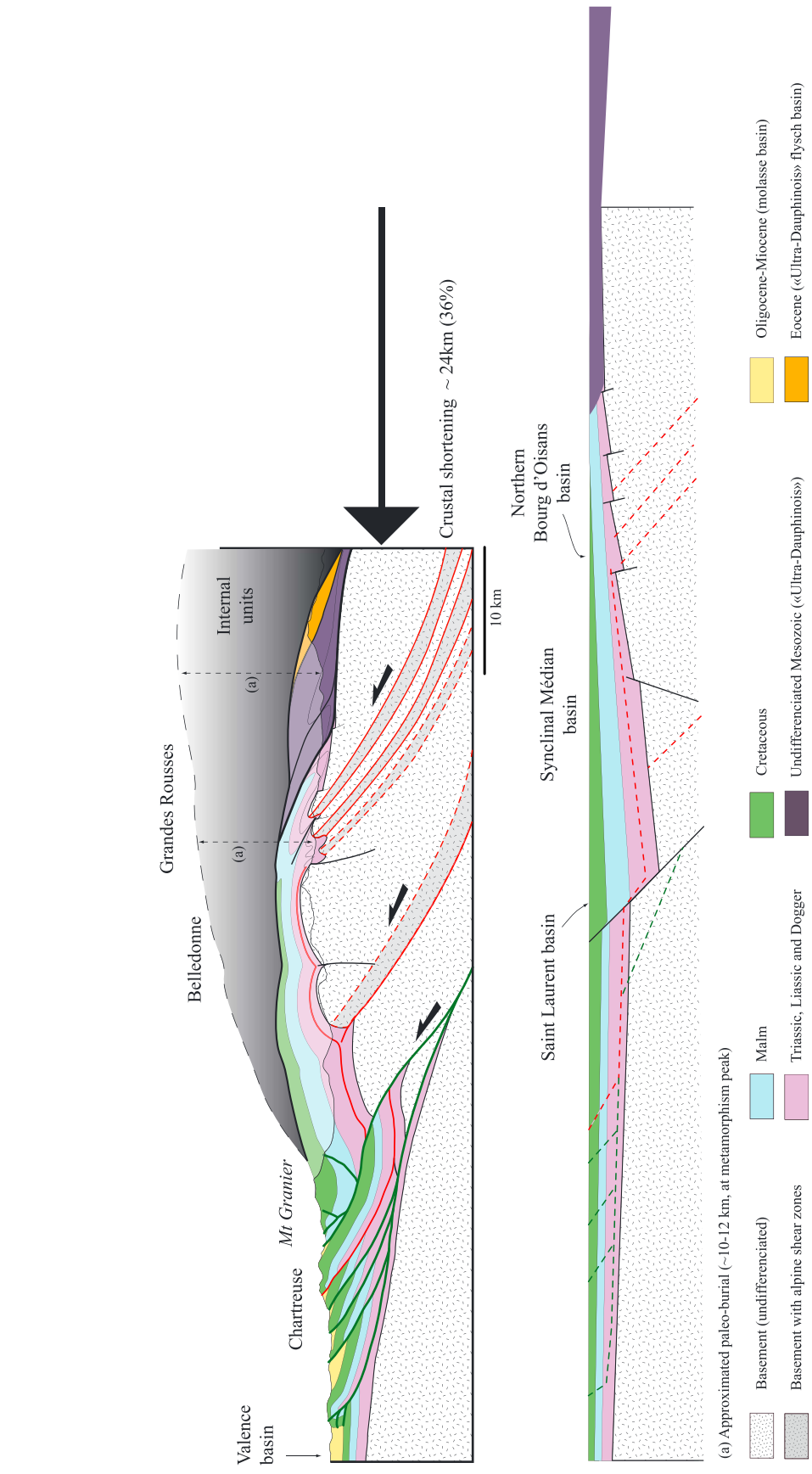

Figure 4. Balanced cross section through the Chartreuse-Belledonne-Grandes Rousses massifs: the Chartreuse-Grandes Rousses cross section. The subalpine part (Chartreuse) is redrawn from *Deville et al.* [1994] and constrained by seismic data. A total amount of shortening of 26.9 km of shortening is recorded for the whole external zone: 6.6 km for the ECM most likely during Oligocene-early Miocene times, 17.8 km for the subalpine chain whose thrusts root in a décollement within Liassic layers activated by frontal basement thrusts beneath the ECM, except for the red thrust that root above the ECM. The outermost thrust is considered to belong to the Jura belt (2 km of shortening). A Mesozoic normal fault has been represented on the restored section based on thickness variations across the easternmost thrust in the subalpine chain. This implies a rather long-lived normal displacement during Mesozoic times. In dark purple are represented detached Mesozoic (mainly Jurassic, ultra-Dauphinois) layers that were not taken into account in the crustal restoration of the Alpine shortening. They most probably witness a (early?) stage of thin-skinned tectonics. See text for explanation and discussion.

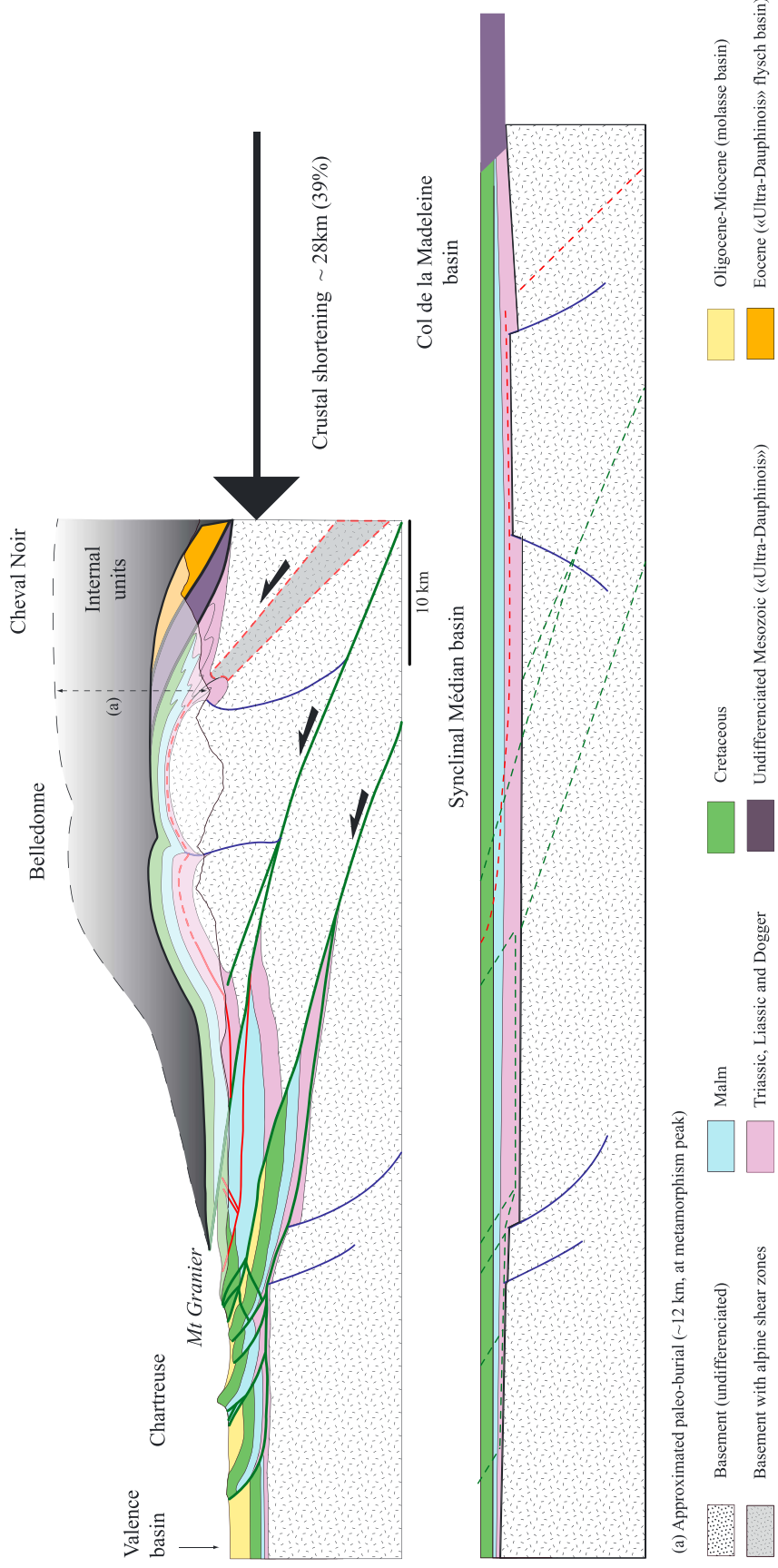

Figure 5. Balanced cross section through the north Chartreuse-Belledonne massifs: the Chartreuse-Belledonne cross section. The section is redrawn, for the subalpine chain part, from *Deville and Chauvière* [2000]. A total of 27.9 km of shortening is recorded for the whole external zone: 7.2 km for the ECM most likely during Oligocene-early Miocene times, 18.7 km for the subalpine chain whose thrusts root in a décollement within Liassic layers activated by frontal basement thrusts beneath the ECM, except for the red thrust that root above the ECM. The outermost thrust is considered to belong to the Jura belt. In dark purple are represented detached Mesozoic (mainly Jurassic, ultra-Dauphinois) layers that were not taken into account in the crustal restoration of the Alpine shortening. They most probably witness a (early?) stage of thin-skinned tectonics. See text for explanation and discussion.

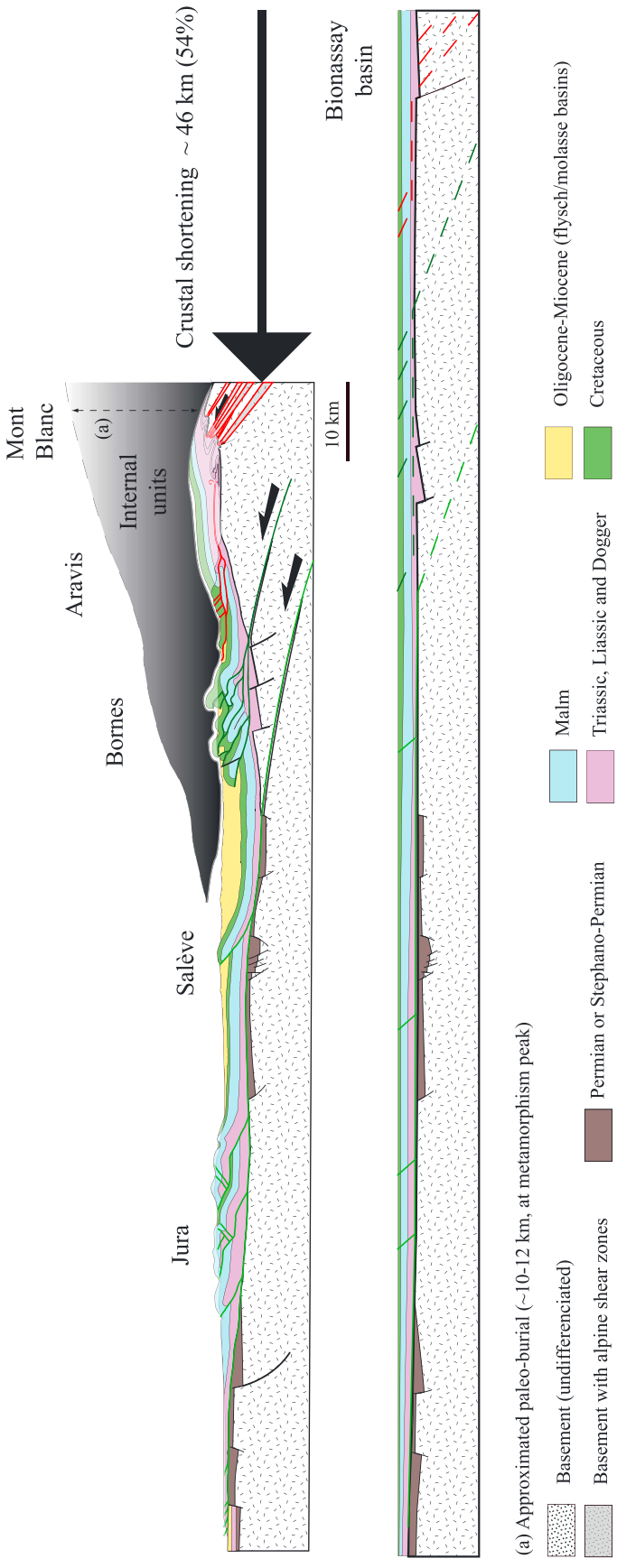

Figure 6. Balanced cross section through the Jura-Bornes-southwestern Mont Blanc massifs: the Bornes-Mont Blanc cross section. The subalpine (Bornes) and Jura parts are redrawn from *Affolter et al.* [2008] and partly constrained by seismic data. For the Bresse graben and Jura relationships, see also *Bergerat et al.* [1990] and *Philippe et al.* [1998]. A total of about 46 km of shortening is recorded for the whole external zone: 3.1 km for the ECM during Early Miocene times characterized by basement Alpine shear zones in the Mont Blanc massif above which the cover is disharmonically folded [*Epard*, 1990], 17 km for the subalpine chain whose thrusts root in a décollement within Liassic layers activated by basement thrusts beneath the northern Belledonne massif, 25.9 km for the Jura whose thrusts root in the Triassic evaporites activated by lower Belledonne basement thrusts. The Mont Blanc shear zones are located beneath an inherited Liassic basin. East of the Bornes massif, i.e., in the Aravis massif, the shortening observed in the field has been rooted in the lower Jurassic layers above the Mont Blanc units and their disharmonic basal sedimentary rocks (Triassic and lower Jurassic). See text for explanation and discussion.

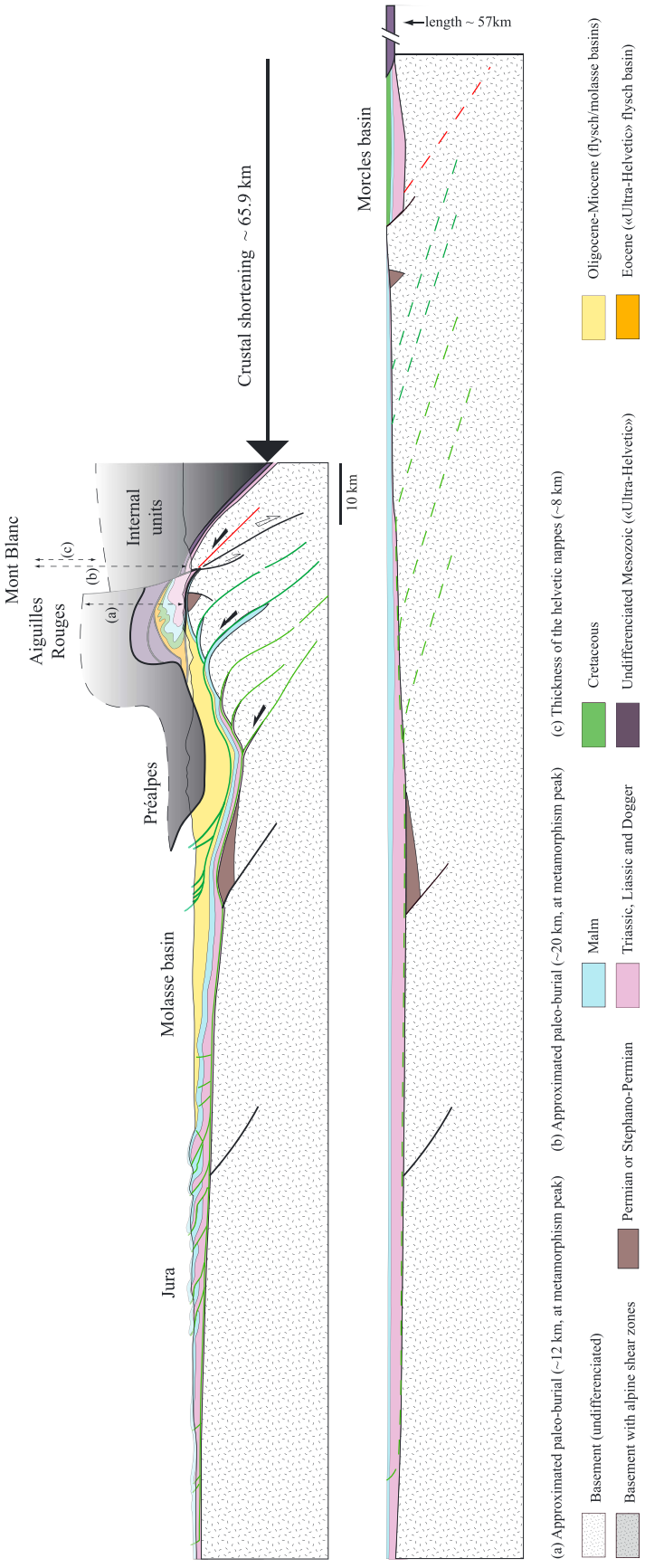

Figure 7. Balanced cross section through the Jura-Préalpes-Aiguilles Rouges-Mont Blanc massifs: the Prealpes-Mont Blanc cross section [*Burkhard and Sommaruga*, 1998]. The Jura and molasse basin parts were constrained by seismic data. A total amount of shortening of about 65.9 km is recorded for the whole external zone: 10.6 km for the ECM during Early Miocene times characterized by large basement Alpine shear zones in the Mont Blanc massif above which the cover (Morcles nappe) is disharmonically folded and sheared, 26 km for the subalpine chain that affect the Tertiary shallow marine to freshwater clastics (NAFB) whose thrusts root in a décollement within Tertiary layers activated by basement thrusts beneath the Aiguilles Rouges, 29.3 km for the Jura whose thrusts root in the Triassic evaporates activated by lower Aiguilles Rouges basement thrusts. The Mont Blanc shear zones are located beneath an inherited Liassic basin. The sedimentary nappes above the Morcles nappe (dark purple, ultra-Helvetic) witness a (early?) stage of thin-skinned tectonics. See text for explanation and discussion.

cover. It is noteworthy that the Grenoble normal fault is not only a Liassic fault but was also active during upper Jurassic (Figure 3).

Moreover, the cover deformed dysharmonically above "basement antiforms" that actually reflect cumulated continuous shortening accommodated by basement shear zones (Figure 8a). Thus, there is no need for major décollement between the cover and the basement. Below the Eocene turbidites unit, however, in the eastern part, small cover units are detached from their basement. In the ECM, the upper part of the cover cannot be unambiguously drawn as it has been strongly eroded (Figure 3). It is probable that the upper Mesozoic series have been eroded during the Pyrenean phase (Eocene in age) as the Cenozoic formations unconformably overlie the basement in southern Oisans [*Ford*, 1996].

Further west, in the Vercors fold-and-thrust belt, cover units are detached in Liassic series (or upper Triassic) at the front of basement thrust ramps [*Deville et al.*, 1994]. There, the cover was affected by several normal faults (Figure 3) that may have initiated during Mesozoic times and were reactivated during the Oligocene before the fold-and-thrust-belt formation.

3.2. The Chartreuse-Grandes Rousses Cross Section

The subalpine part of the cross-section part (Figure 4) has been redrawn from *Deville et al.* [1994] in *Philippe et al.* [1998]. There, several thrusts deformed the sedimentary cover over a décollement in the Liassic series (or upper Triassic series) and the associated shortening corresponds to the displacement along two basement thrusts. It is noteworthy that the thrust spacing and the belt width are much smaller than in the previous cross section (Vercors, Figure 3) and mainly controlled by sedimentary rock thickness, much higher in the Vercors than in the Chartreuse massif, and by the rheological properties of the décollement level [*Philippe et al.*, 1998]. The total amount of shortening on these thrusts is about 17.8 km and started during Burdigalian-Langhian times [*Arnaud*, 1975].

We propose that one of the thrusts (in red in Figure 4, Mt Granier) roots in the Liassic layers above the ECM basement, following *Deville et al.* [1994]. Thus, this thrust was activated before the ECM uplift and the frontal basement thrust activation. However, further east, no evidence of any significant décollement in the cover can be observed in the field. Indeed, in our section, the cover deformed dysharmonically over the basement shear zones that correspond to two basement highs of the Grandes Rousses redrawn from *Bellahsen et al.* [2012]. The flat surface at the cover base above the Belledonne high (décollement) was rooted above the basement shear zones located between the Grandes Rousses and Belledonne massifs (Figure 4). This means that the basement shear zone propagated into the cover, though it is poorly documented in the field because of the ductile behavior of the cover and exposure conditions. The amount of shortening along this early thrust observed at surface in the fold-and-thrust belt is quite important, around 3 km. Thus, it is likely that some of this amount (at least half of it) can be associated to the basement thrust that apparently offset the (red) flat (Figure 4).

As mentioned above, in the ECM, three basement shear zones (two cropping out and one hidden) most likely shortened the crust. The amount of shortening accommodated by these structures is about 6.6 km. Thus, the total amount over the external zone in this area is about 26.9 km: an amount of shortening of 2.5 km is attributed to the Jura phase, as the outermost thrusts are in the southern continuity of the Jura belt (Figure 1 and Table 1).

Several Mesozoic normal faults are attested by thickness variations (Figure 4): the main one is the Saint Laurent (du Pont) normal fault. This normal fault has been inferred from the section in *Deville et al.* [1994] redrawn here, where a significant Mesozoic thickness variation occurs across the easternmost fault within the subalpine belt (Figure 4). We consequently interpret this thrust as the propagation in the cover of a reactivated inherited Liassic normal fault. In the restored section, the normal fault controls thickness variations up to the Cretaceous layers. This implies a long-lived fault activity having continued after the end of the Ligurian rifting (Liassic to Dogger times) and which may correspond to the Cretaceous extension recorded further south [e.g., *Homberg et al.*, 2013; *Bertok et al.*, 2012] and north (Valais domain [*Handy et al.*, 2010, and references therein]). Other normal faults are the "Synclinal Médian" and northern Bourg d'Oisans faults, as well as other minor faults in and around the Grandes Rousses massif (Figure 4). We found no evidence for their Alpine reverse reactivation.

As in the previous cross section (Figure 3), east of the section, detached units of Liassic rocks considered as ultra-Dauphinois are overthrusted by the Eocene flysch unit.

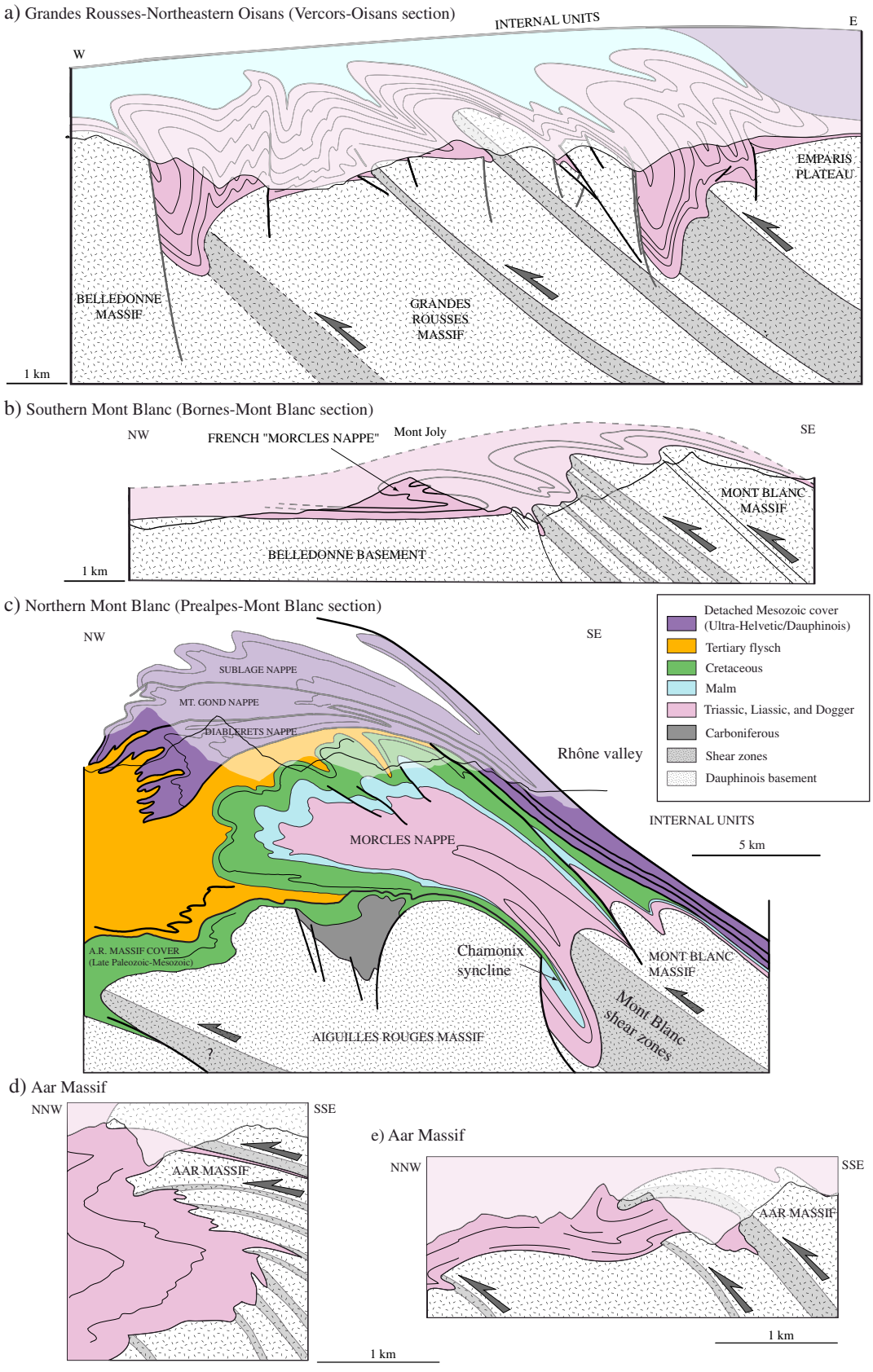

Figure 8

Table 1. Shortening and Amounts of Shortening for Each Section During Each Phase[a]

	Total Amount of Shortening (km)	Uncertainty (km)	ECM (km)	Subalpine (km)	Jura (km)	Shortening ECM (%)	Shortening Crust (%)	Shortening External Zone (%)
Vercors-Oisans	28	±2	11.5	16.5	0	16.1	27.5	20.6
Chartreuse-Grandes Rousses	26.9	±2	6.6	17.8	2.5	14.8	35.9	27.1
Bauges-Chatelard	27.9	±2	7.2	18.7	2	18.5	39.6	27.5
Bornes-Mont Blanc	46	±5	3.1	17	25.9	29.1	54.6	24.0
Prealpes-Mont Blanc	65.9	+10, −1	10.6	26	29.3	38.3	57.2	27.1
Prealpes-Aar	~69	?	12	31	26	40	67	29

[a]The uncertainty for the Préalpes-Mont Blanc section is from *Burkhard and Sommaruga* [1998]. The uncertainty for the Préalpes-Aar section is unknown, as it is not balanced in *Burkhard* [1988]. However, we consider the value as an order of magnitude. Uncertainty for the Vercors-Oisans section is from *Bellahsen et al.* [2012] and mainly due to uncertainty of Triassic length in ECM and at the transition subalpine chain/ECM. The same uncertainty is used for the Chartreuse-Grandes Rousses and Chartreuse-Belledonne section. For the Chartreuse-Grandes Rousses and Chartreuse-Belledonne sections, the frontal thrust has been considered as belonging to the Jura belt (see Figure 1). The shortening is calculated in three different ways (see Figure 12).

3.3. The Chartreuse-Belledonne Cross Section

In this cross section (Figure 5), the western part (Chartreuse and west Belledonne) was redrawn after *Deville and Chauvière* [2000]. There, several thrusts in the cover rooted in two basement thrusts. In this cross section built after seismic data, one may find the best evidence for the allochthonous nature of the ECM, the basement clearly overthrusting the sedimentary cover of the subalpine belt. The amount of shortening accommodated by these basement thrusts is about 18.7 km.

As in the previous section (Figure 4), a thrust in the eastern part of the folded belt (in red, Figure 5, Mt Granier) roots within the Liassic layers but above the Belledonne basement high. The flat is thus drawn until east of Belledonne where it roots in a basement shear zone. Within the Belledonne massif, a vertical fault (Figure 5) is mapped out in the field [e.g., *Marquer et al.*, 2006]: it is most probably an inherited Jurassic normal fault (bounding the Synclinal Median basin as in the previous cross section, Figure 4) that was dipping west and was not significantly reactivated but deformed and verticalized.

There are three main inherited normal faults: one hidden below the subalpine belt (observed on seismic lines [*Deville and Chauvière*, 2000]), the normal fault east of the Synclinal Médian basin (see above), and the normal fault that controls the Col de la Madeleine basin (Figure 5).

The amount of shortening associated to the deformation within the ECM is about 7.2 km. Thus, the total amount over the external zone in this area is about 27.9 km: an amount of shortening of 2 km is attributed to the Jura phase, as the most external thrusts are in the southern continuity of the Jura belt (Figure 1 and Table 1).

Here again, below the frontal penninic thrust, an allochthonous Eocene flysch unit overthrusted a unit made of Liassic series itself detached from its basement in the eastern part (ultra-Dauphinois).

3.4. The Bornes-Mont Blanc Cross Section

The fold-and-thrust belt part of this cross section (Figure 6) was redrawn after [*Affolter et al.*, 2008], from the western end of the section to the Aravis massif. It consists of two parts: the Jura and the subalpine chains. In the former, the amount of shortening is about 25.9 km and is accommodated by numerous thrusts that rooted in Triassic evaporites [*Affolter et al.*, 2008]. The décollement has been subsequently deformed below the internal Jura by later high-angle basement thrusts related to inversion of permo-carboniferous basins (e.g., *Lacombe and Mouthereau* [2002]; Figures 6 and 7). The décollement within the Triassic is connected to a basement thrust as in *Burkhard and Sommaruga* [1998]. In the latter (subalpine chains), an amount of shortening of 17 km is recorded

Figure 8. Detailed cross sections showing the basement-cover relationships in the different ECM. (a) Along the Vercors-Oisans section, the cover is disharmonically folded above basement shear zones [*Bellahsen et al.*, 2012]. (b) Along the Bornes-Mont Blanc section, the cover is disharmonically folded above basement shear zones: the Mont Joly (Figure 1) structure is from [*Epard*, 1990], who interpreted it as the "French" Morcles nappe. In the field, clear Alpine shear zones can be observed and correspond to the mapped basement top "folds". (c) Along the Préalpes-Mont Blanc section, the Morcles nappe is interpreted as the Mont Blanc cover [*Escher et al.*, 1993]. The Morcles nappe geometry and Aiguilles Rouges massif structure is from *Escher et al.* [1993]. We have modified the original figure to display the Mont Blanc shear zones and the probable Chamonix normal fault also drawn in *Burkhard and Sommaruga* [1998]. (d and e) Basement-cover relationships in the Aar massif from *Ramsay et al.* [1983] and *Heim* [1921], respectively. Note that each inverted basement "fold" limb correspond to basement shear zones as observed in Figures 8a–8c.

and accommodated in a basement thrust. Such structural choice is made for along-strike structural consistency with the other cross sections. Indeed, it is clear that further south the subalpine chains are due to the activation of a décollement by basement thrusts beneath the ECM (Figures 4 and 5, for example).

However, in Figure 6, thrusts in the Aravis massif have not been rooted in any basement thrust for several reasons. Firstly, basement thrusts are not clearly exposed in the field. Secondly, in the western Belledonne massif, as in northwestern Aiguilles Rouges massif, sedimentary rocks display top-to-the-NW thrusts and NW verging folds. These thrusts probably root near basement shear zones further east such as in the previous cross sections. Such structures are then older than the ECM shortening and uplift, or coeval with their early deformation.

In the easternmost part of the section, the SW Mont Blanc structures consist of NW verging basement shear zones observed in the field and associated recumbent folds in the cover. There, the cover is not detached over the basement (Figure 8b) and displays similar geometries as in the Morcles nappe (Figure 8c) [*Epard*, 1990; *Escher et al.*, 1993], in northern Oisans (Figures 3 and 8a) [*Bellahsen et al.*, 2012], and in the Aar massif (Figures 8d and 8e) [*Ramsay et al.*, 1983, and references therein]. The associated amount of shortening is about 3.1 km. Thus, the total amount over the whole external zone is about 46 km (Table 1).

3.5. The Prealpes-Mont Blanc Cross Section

This cross section (Figure 7) has been redrawn from *Burkhard and Sommaruga* [1998]. Thus, we will only sum up the main implications. The total amount of shortening is about 65.9 km (Table 1), among which 29.3 km is linked to the three frontal basement thrusts of the lower part of the Aiguilles Rouges massif, attesting for the shortening in Jura fold-and-thrust belt that shortened above a décollement in the Triassic layers [*Burkhard and Sommaruga*, 1998; *Affolter et al.*, 2008]. The structures in the Aiguilles Rouges massif have been drawn as basement thrusts, although they might have been more distributed shear zones (e.g., *Steck et al.* [1997], see discussion part).

The amount of shortening within the Tertiary sedimentary rocks of the NAFB (NW of the Préalpes, structures equivalent to the subalpine chains further SW) is about 26 km above a décollement in the Tertiary series and rooted in two thrusts of the upper Aiguilles Rouges.

The Morcles unit is a recumbent anticline that represents the cover of the Mont Blanc massif, where an amount of shortening of 10.6 km is recorded. The Morcles nappe is thus not strongly detached from its basement, although it has been slightly translated toward the NW as attested by the intense shearing of its overhanging limb [*Escher et al.*, 1993]. In Figure 8c, adapted from *Escher et al.* [1993], we added the Mont Blanc shear zones [*Leloup et al.*, 2005; *Rolland et al.*, 2008] and the inherited Jurassic normal fault in the Chamonix syncline (see also [*Boutoux et al.*, 2014]), although it does not clearly crop out in the syncline. However, this normal fault is necessary to explain the cover thickness difference above the Aiguilles Rouges massif (thin series) and above the Mont Blanc massif (thick series).

The two upper sedimentary nappes, the Diablerets and the Wildhorn nappes, consist of detached units that represent the cover of more internal crustal domains (ultra-Helvetic).

4. Discussion

Here we present a synthesis of the structural style of the external zone of the Western Alps in order to provide a structural map consistent at the scale of the whole orogenic domain. Then, the sequence and amount of shortening can be determined, as well as average estimates of exhumation/uplift rates. The shortening sequence is also used to produce palinspastic maps from the SW to the central Alps at four key periods of the Tertiary evolution. Finally, a restoration of the Mesozoic proximal continental margins is proposed and discussed.

4.1. Structural Style

On the cross sections presented above, the shortening that is recorded in both the Jura and the subalpine chains is connected to displacement along basement thrusts below ECMs. Evidence for such a geometry can be found in the subalpine chains on seismic lines (see interpretation of *Deville and Chauvière* [2000] for the Western Alps and *Pfiffner et al.* [1997] and *Steck et al.* [1997] for the central Alps) where the basement clearly overthrusts the sedimentary cover of the fold-and-thrust belt. Alternatively, the subalpine chains could have been emplaced before the ECM uplift, and if so, their shortening would have to be rooted above them. This sequence of tectonic events was proposed by *Leloup et al.* [2005] or *Affolter et al.* [2008], for example, and requires the subalpine chain shortening to be older than the ECM uplift.

This model was supported by uplift ages in the Mont Blanc and Aiguilles Rouges massifs not older than 22 Ma. Moreover, the Morcles nappe is sometimes interpreted as equivalent of the subalpine chains [*Doudoux et al.*, 1982; *Leloup et al.*, 2005]. However, in the south, at the Oisans latitude, the subalpine chain emplaced about 15 Ma ago, i.e., significantly younger than the exhumation of the Oisans ECM that started before 27 Ma [*van der Beek et al.*, 2010]. North of the Mont Blanc massif, the lateral equivalent to the subalpine chains, i.e., the Subalpine Molasse thrust, is dated back to 15–20 Ma [*Burkhard and Sommaruga*, 1998], while the Mont Blanc shortening started around 30 Ma [*Cenki-Tok et al.*, 2013]. Thus, the timing of ECM and Subalpine shortening are well-constrained and likely express the sequential involvement of inner ECM basement units followed by the subalpine chain. As a consequence, the subalpine chain appears kinematically related with frontal basement thrusts. This interpretation is similar to that proposed by *Burkhard and Sommaruga* [1998], redrawn in Figure 4, but also by *Ménard and Thouvenot* [1987], *Guellec et al.* [1990], and *Mugnier et al.* [1990] around the ECORS profile location. The subalpine belts are represented in dark green in Figure 9.

If the subalpine chains are linked to ECM basement thrusts, then the same should be for Jura, as it is younger than the subalpine chains and the ECM uplift (compare ages in *Arnaud* [1975] and *Philippe et al.* [1998] and ages in *Kalin* [1997], *Bolliger et al.* [1993], *Steiniger et al.* [1996], *Becker* [2000], and *Rolland et al.* [2008]). This Jura unit is represented in light green in Figure 9.

The basement structures in the frontal ECM are named "basement thrusts" but may very well be localized shear zones [e.g., *Steck et al.*, 1997]; many of them unfortunately do not crop out. In the "internal" ECM (Mont Blanc, Oisans), the structures accommodating shortening are indeed shear zones. In the frontal ECM, the structures might be more localized as they activate upper décollements (at the base of the sedimentary cover): they are probably brittle-ductile thrusts/shear zones, more localized than the Mont Blanc shear zone but more distributed than a cataclastic thrust.

Few units in the subalpine chains cannot be explained by the activation of a décollement due to basement thrusts below the frontal ECM. Indeed, several thrusts branch on a décollement above the ECM (Figure 10) as shown in *Deville et al.* [1994] and redrawn in Figures 4 and 10d, in *Deville and Chauvière* [2000] and redrawn in Figures 5 and 10c, and in *Affolter et al.* [2008] and redrawn in Figures 6 and 10b. These (small) units suggest that the ECM cover was slightly detached from the basement, which justifies considering it as a unit distinct from the subalpine one in a strict sense. However, further north, around the northeastern Aiguilles Rouges massif, the cover is thin and not detached from its basement (Figures 7 and 10a) [*Escher et al.*, 1993]. Thus, this unit must terminate in this area and is restricted to the "French Alps." Similarly, further south on the section south of Grenoble (Figures 3 and 10e) from *Deville et al.* [1994], this unit does not appear and probably also terminates around the southern Belledonne massif (south of the Rochail massif), as we find no evidences for such a unit in the field between Gap and Grenoble (Figure 1).

The geometry of the thrusts bearing this unit is compatible with the geometry proposed in *Epard and Escher* [1996], where sedimentary nappes are related to basement shortening along shear zones that are located several kilometers toward the internal zones. The faults belonging to this unit are represented in red in Figure 9. Since the subalpine chain has later deformed this unit, it could hardly be represented in map view at this scale.

Thus, our analysis proposes a new unit, named "Aravis-Granier" unit, corresponding to a part of the sedimentary cover whose shortening is attested by folds and thrusts that branch on a décollement within the Liassic series above the ECM (Figure 9). However, this unit is not observed either north of the Mont Blanc massif or southwest of the Belledonne massif. This along-strike variation in the structural style may be explained by the depth of underthrusting of the European crust and the extent of the internal units. In the north, the crust was buried down to about 20 km (in the Mont Blanc for example). We here propose that, at this depth and corresponding temperature (400°C [*Rolland et al.*, 2008]), the crust was very weak and detached in the middle lower crust (Figure 11d; see also further down). As a consequence, both the basement and its cover could be shortened in the same way without any significant décollement as there would be little rheological contrast between the basement and the cover (Figure 11d). Southwest of the Mont Blanc, the Belledonne massif was probably buried down to less than 10 km, as the Aiguilles Rouges massif [*Leloup et al.*, 2005], probably due to their frontal position. Such burial did not induce a strong weakening of the crust (Figure 11b). Then, the sedimentary layers were probably much weaker than the deforming basement, and as a consequence, part of the cover detached from the basement. In the

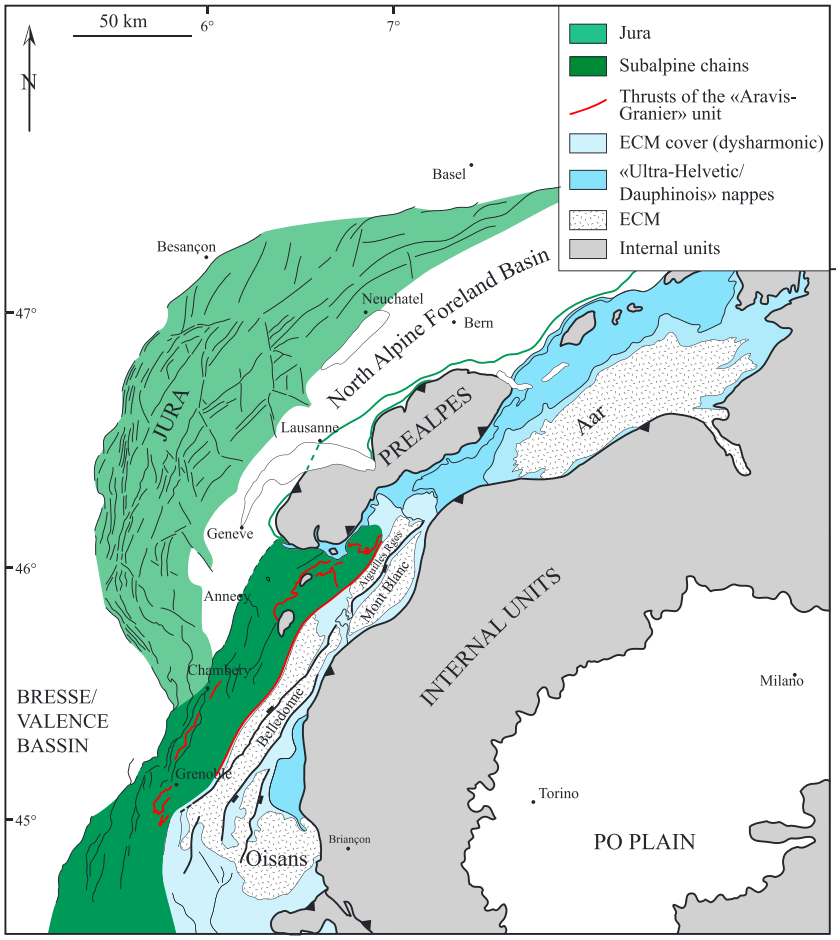

Figure 9. New structural map of Western Alps. Colored areas correspond to different units. Light green represents Jura, and dark green represents subalpine chains. By subalpine chains, we mean fold-and-thrust belts that are due to the activation of a basal décollement activated by basement frontal thrusts beneath ECM. Light blue areas represent the Helvetic-Dauphinois sedimentary nappes or cover of the ECM that are autochthonous (western limb in northeastern Aiguilles Rouges), disharmonically folded above basement shear zones (Oisans cover and Mont Joly), and/or slightly sheared above their basement (Morcles). In darker blue are the early detached sedimentary units that represent the cover of ultra-Dauphinois/helvetic basement. Finally, in red, we have represented the thrusts that correspond to the detached part of the ECM cover; i.e., upper part of the Mont Joly unit for example. In other words, along the Préalpes-Mont Blanc section (NE section), the whole Mesozoic cover of the Mont Blanc is represented by the Morcles nappe, while along the Bornes section (SW Mont Blanc), the Mont Joly (French Morcles) is only made of the lower Jurassic layers. The rest of the cover is displaced and composes the "Aravis-Granier" unit.

southwest Belledonne massif, the burial was lower than in the northeast Belledonne massif but the cover was not detached (see above). There, the amount of shortening is much lower than further north. As a consequence, the shortening east of Belledonne was not significant enough to imply a décollement above Belledonne as further north. The presence of a detached unit at the ECM front is thus ascribed to a combination of particular crustal rheology and significant amount of shortening, two parameters themselves probably not independent from each other.

In light blue in Figure 9, the ECM cover is not significantly detached over its basement as shown by [*Bellahsen et al.*, 2012] (pink in Figures 3–7 and 10). This includes the Morcles nappe, NE of the Mont Blanc massif (Figure 8c) [*Escher et al.*, 1993], and the Mont Joly, its French equivalent SW of the massif (Figure 8b) [*Epard*, 1990]. Recent ages of Mont Blanc deformation around 30 Ma [Cenki-*Tok et al.*, 2013] confirm the structural interpretation invoking that the Morcles nappe is the Mont Blanc cover; these ages are synchronous with earliest deformation in the Morcles nappe at 30 Ma [*Kirschner et al.*, 1996]. The Morcles recumbent anticline was then emplaced over the Aiguilles Rouges.

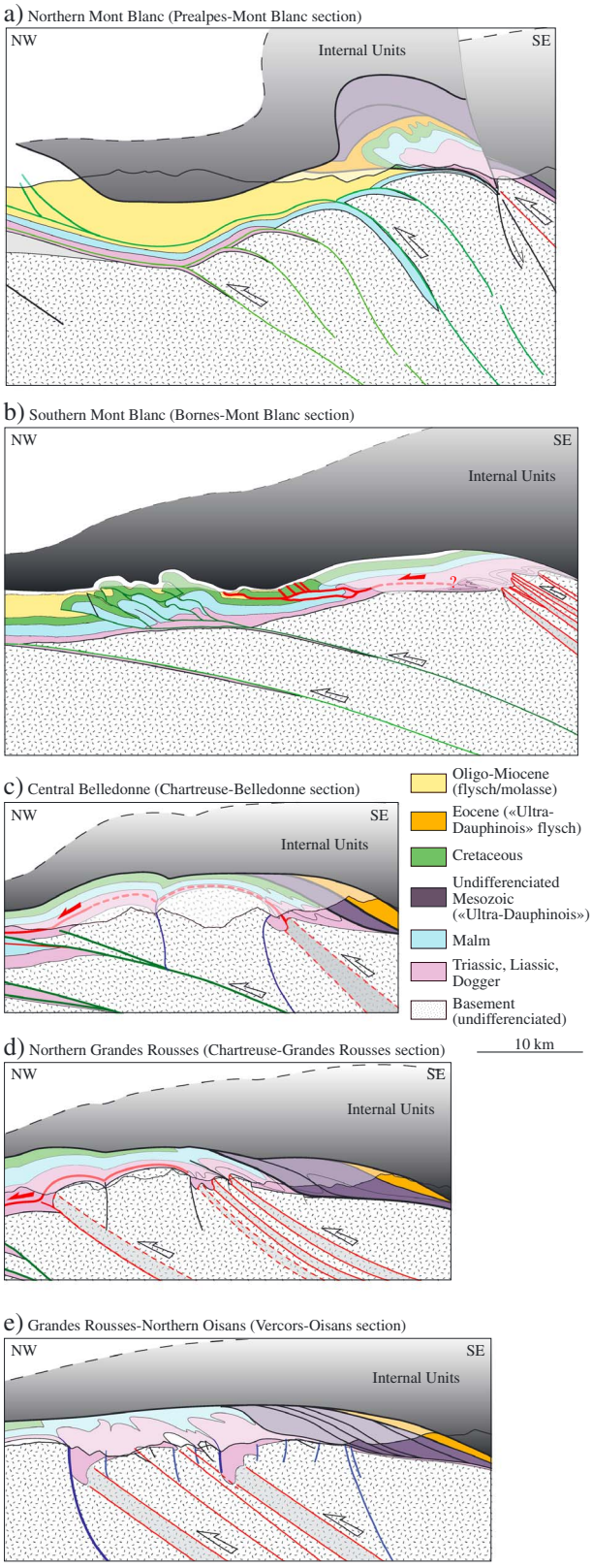

Figure 10. Zooms of the ECM-subalpine chain relationship from cross sections from Figures 5–9. Note the presence of the red thrust (Aravis--Granier unit): the upper part of the cover of the Belledonne massif is detached from the rest of the cover, except in the northernmost and the southernmost cross sections.

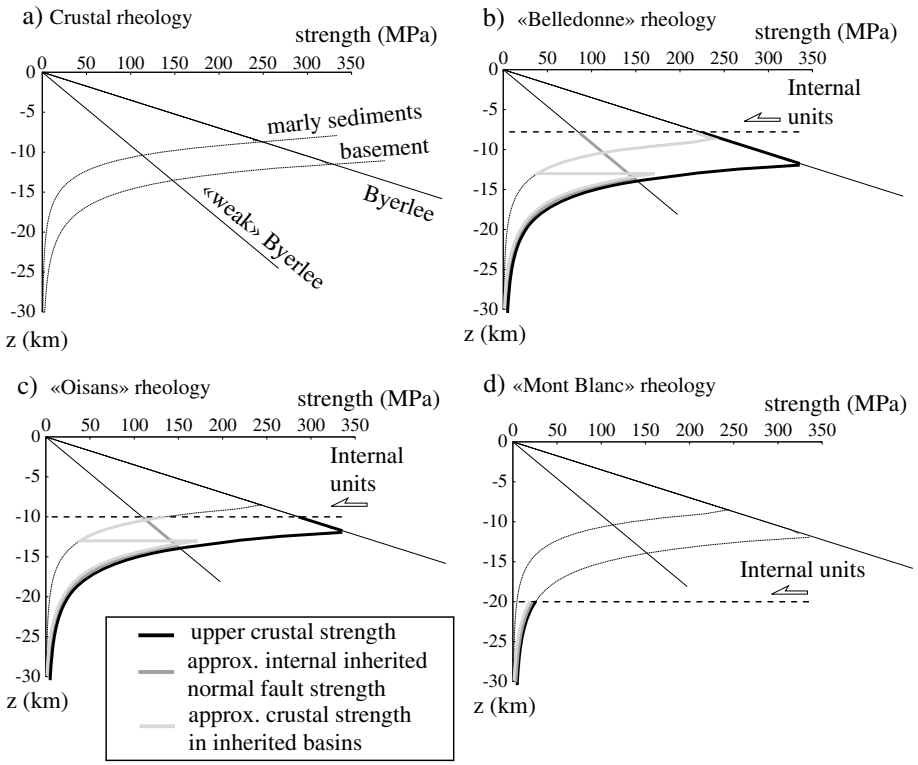

Figure 11. Rheology of the crust. (a) Before the collision (see *Bellahsen et al.* [2012] for details). "Weak byerlee" is taken for the inherited Liassic normal fault internal strength. "Marly sediments" is for the Liassic sedimentary rocks in the inherited basins. (b) During the collision for the Belledonne part of the Chartreuse-Grandes Rousses and Chartreuse-Belledonne sections. (c) During collision for Oisans massif on the Vercors-Oisans section. The crustal strength with an inherited basin is lower than both the crust without basin and the inherited normal faults internal strength. (d) During collision for the Mont Blanc massif on the Bornes-Mont Blanc and the Préalpes-Mont Blanc sections. The crust is ductile and very weak.

Further south (around the Grandes Rousses and north of the Oisans massif), the structural style is similar but with less shortening (compare Figures 3–7). All these areas similarly show recumbent anticlines in the sedimentary cover and are associated with distributed shear zones within the basement (Figure 8).

Finally, the sedimentary nappes above the Morcles unit, i.e., the Diablerets and the Wildhorn nappes (Ultra-Helvetic) are most likely detached over their basement as in *Burkhard and Sommaruga* [1998]. Similar geometries can be found north of the Oisans massif. The detached Liassic units in Figures 3–5 may be equivalent to the ultra-Helvetic nappes mentioned above. These units have been represented in dark blue in Figure 9 (purple in Figure 10). These ultra-Dauphinois/Helvetic nappes probably emplaced during the early Alpine collision, most likely during early Oligocene [e.g., *Burkhard and Sommaruga*, 1998; *Ceriani et al.*, 2001; *Simon-Labric et al.*, 2009; *Bellanger et al.*, 2014]. These cover units are the only ones that could possibly be unrelated to basement shortening. Beside these units, in the Alpine external zone, all the shortening observed in the cover (fold-and-thrust-belt and ECM cover) corresponds to basement shortening.

4.2. Amounts of Shortening

According to the above results, the shortening recorded in the external zone is related to basement shortening and therefore reflects the presence of a deep crustal detachment. Here we present a summary of amount of shortening estimates (Figure 12 and Table 1).

Our estimates of the frontal basement thrust displacements mainly arise from balanced cross sections of fold-and-thrust belts in the literature, and their northward increase is consistent with previous works [*Ménard and Thouvenot*, 1987; *Sinclair*, 1997]. Our estimate of the total amount of shortening through the external zone along the ECORS profile is similar to those proposed by *Mugnier et al.* [1990] and by *Guellec et al.* [1990]. We

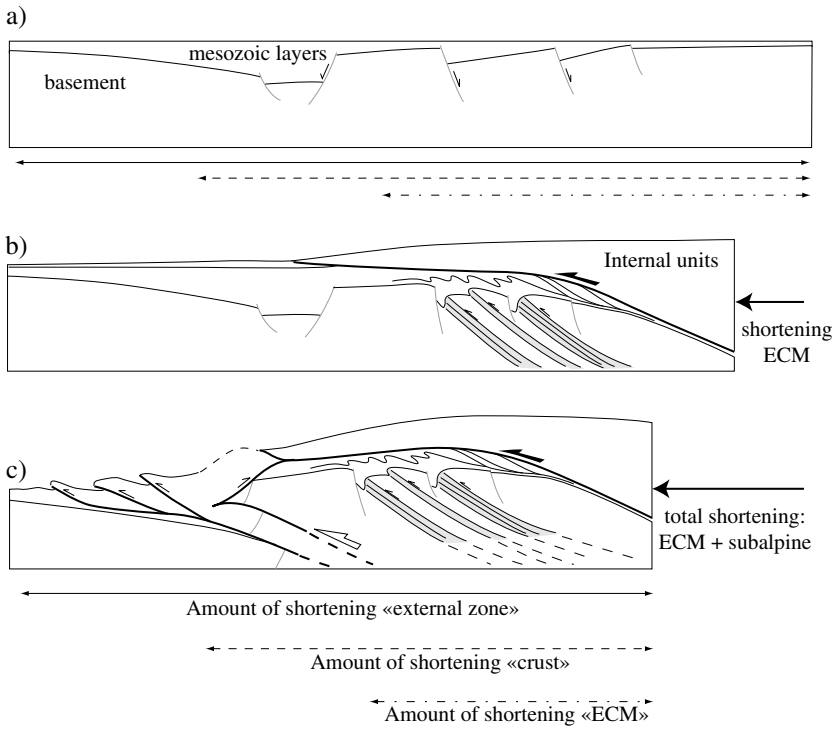

Figure 12. Amounts of shortening measurements. Schematic structures of the Oisans section during (a) preorogenic times, (b) early burial beneath internal units with ECM shortening, and (c) late subalpine chain shortening, from *Bellahsen et al.* [2012]. The amount of shortening "ECM" is calculated considering the initial and final width of deformed ECM, i.e., the extent of the main basement shear zones. The amount of shortening of the crust (ECM plus frontal thrusts) is calculated considering the initial and final width of the crust, i.e., from the Penninic Frontal Thrust (PFT) to the outermost buried basement thrust. The amount of shortening "external zone" is calculated considering the initial and final width of the whole external zone, i.e., from the PFT to the frontal cover thrust.

found that the amount of shortening over the entire external zone increases from 28 km in the south (Vercors-Oisans section) to 65.9 km in the north (Prealpes-Mont Blanc section) (Table 1). This is due to (1) variations in the amount of shortening in the ECM, (2) an increase in the amount of shortening in the subalpine chains, and (3) an increase due to the Jura northward.

The whole external zone shortening ranges between 20% in the south and around 30% in the north, consistent with the range of shortening values typically observed in the Alps and other young peri-Tethyan orogens [e.g., *Mouthereau et al.*, 2013]. However, it is noteworthy that this variation is not as large as the variation of the amount of shortening (Table 1). This is due to the contribution of locally more thin-skinned deformation featured in the Jura that increases the total amount of shortening as well as the original width of the restored external domain. The width enlarged because of the presence of both an efficient décollement in Triassic layers and the thick NAFB [e.g., *Fillon et al.*, 2013], allowing efficient stress transfer without much internal strain. This outlines a stronger basement relative to cover in the foreland.

The shortening considering the basement only (%, Figure 12) increases northward more than the shortening calculated over the whole external zone (Table 1). This is mainly due to the increase in amount of shortening along the frontal thrusts from south to north. This means that, northward, the amount of crustal shortening increases (most likely because of more convergence in the north) and is more localized in space. Note, however, that this does not mean that the deformation at smaller scale is more localized in terms of deformation mechanisms. This is actually the opposite: toward the north, in the Mont Blanc [*Rolland et al.*, 2008] and Aar massifs [*Marquer*, 1990], the deformation observed in the field is more distributed than in the south [*Bellahsen et al.*, 2012]. In the north the deformation is clearly ductile, while it is only brittle-ductile in the south. This tendency is of course also clear from the P,T conditions: the deformation occurred at about 300–350°C and around 3 kb in the south (Oisans massif [*Jullien and Goffé*, 1993]) and at about 400 to 450°C and 5–6 kb in the north [e.g., *Challandes et al.*, 2008; *Rossi et al.*, 2005].

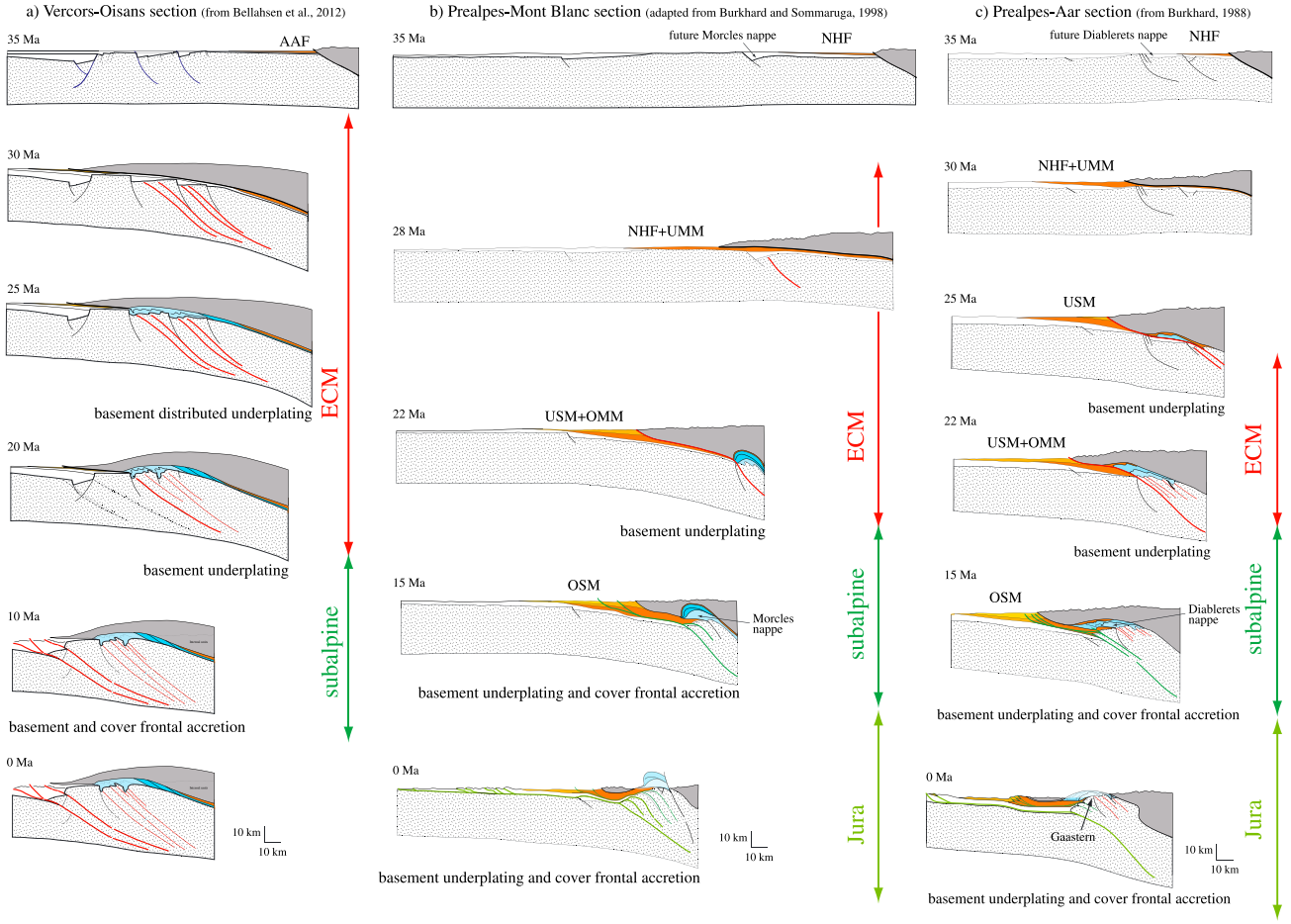

Figure 13. Sequence of shortening for the Vercors-Oisans, the Préalpes-Mont Blanc, and the Préalpes-Aar sections. (a) Shortening sequence for the Vercors-Oisans section from *Bellahsen et al.* [2012]. During the ECM phase (after the deepwater turbidites deposition and burial phase), the crust deformed by distributed underplating in the basement. During the subalpine phase, frontal accretion in the basement produces frontal accretion in the cover and a basal décollement activation. AAF is for Aiguilles d'Arves Flysch. (b) Shortening sequence for the Mont Blanc section deduced from the balanced cross section in *Burkhard and Sommaruga* [1998]. The sequence is quite similar to the one described for the Aar section (Figure 13c). NHF is for north Helvetic Flysch. UMM is for Lower Marine Molasse (German terminology), USM for Lower Freshwater Molasse, OMM for Upper Marine Molasse, and OSM for Upper Freshwater Molasse. (c) Shortening sequence for the Aar section [*Burkhard*, 1988] with age constraints from *Challandes et al.* [2008]. After the phase of deepwater turbidites deposition and subsequent burial beneath the internal units, the orogenic wedge deformed mainly by basement underplating (ECM phase). During the subalpine phase, basement underplating led to frontal accretion of cover units. During the Jura phase, the underplating of the lowest basement unit led to the fast basinward propagation of the orogenic front and the frontal accretion of cover units.

When P,T conditions increase, the deformation is more distributed at the field scale (i.e., rather small scale) but shortening is more localized at the orogen-scale due to change in crustal strength. In other words, under "high" P,T conditions the basement shortening did not "propagate" far toward the foreland, while basement deformation is distributed far toward the foreland under lower P,T conditions, which can be related to the rheology of the crust during collision (Figure 11): a weak crust induces more localized shortening at the orogen-scale.

The cause of these along-strike variation of P,T conditions is still an open question: it may either be due to efficient "subduction/underthrusting" of the crust in the north because of a higher crustal strength and/or more efficient slab pull in the north linked to the complete crustal breakup in the Valais domain (see last section).

4.3. Sequence of Shortening

As described above, the timing of deformation within the different units is as follows: (1) emplacement of the ultra-Dauphinois/Helvetic sedimentary nappes during early Oligocene, (2) shortening of the ECM basement

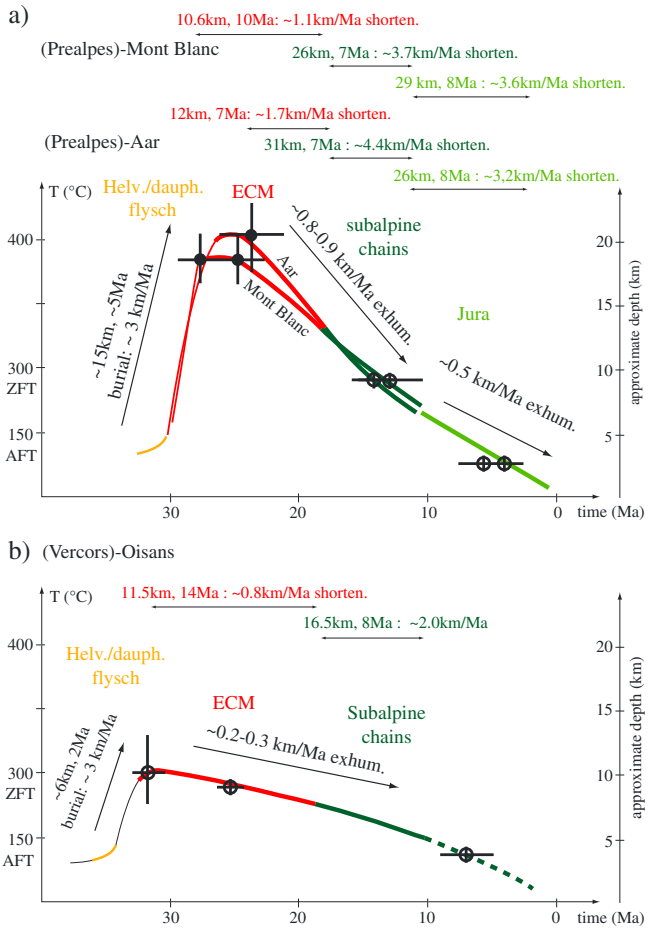

Figure 14. Amounts of exhumation and shortening through time and during the different shortening stage of the sequence: the ECM shortening, the subalpine, and the Jura phases from the data synthesized in Figures 2 and 13 and Table 1. (a) Mont Blanc and Aar data. Exhumation rates are calculated from estimation of depth at various times: metamorphic peak [e.g., *Leloup et al.*, 2005; *Rolland et al.*, 2008; *Challandes et al.*, 2008] and thermochronology (AFT, ZFT) for the retrograde path [see *Vernon et al.*, 2008]. (b) Oisans data. The maximum depth is poorly constrained and estimated from the maximum temperature, around 300°C, that provide a rough estimate of the pressure considering a 30°C/km geothermal gradient. ZFT and AFT data provide other constraints [e.g., *van der Beek et al.*, 2010]. Black circles are pressure constraints; errors bars are thus given for depth. Open circles are constraints on pressure deduced from temperature constraints; errors bars are given for temperature.

and their cover during Oligocene to early Miocene times, (3) activation of both the basement frontal ramps and the décollement below the subalpine chains during Miocene times, and (4) activation of both the lower frontal basement ramps and the décollement below the Jura chain in the north during late Miocene/early Pliocene. This forward sequence is consistent with results from earlier studies [e.g., *Burkhard and Sommaruga*, 1998; *Bellahsen et al.*, 2012].

This forward sequence is, however, variable from north to south. In the south, the ECM shortened in a distributed way (see previous section) during Oligocene times before the deformation localized on the frontal ramp that activated the subalpine chain (Figure 13a). Thus, the deformation of the orogenic wedge is characterized by accretion and thrust stacking from below the wedge ("distributed underplating," Figure 13a) but without wedge widening (frontal accretion) during Oligocene times. This was followed during Miocene times by frontal accretion and wedge widening.

Further north, in the Mont Blanc massif, during Oligocene to early Miocene times, the basement shortened during its underplating below the internal units (Figure 13b). During middle Miocene times and the activation of a fold-and-thrust belt in the foreland basin, the dynamics still consisted of underplated basement units (upper Aiguilles Rouges), while small amounts of frontal accretion occurred within the cover. During the time of Jura formation in late Miocene to early Pliocene, basement units were also underplated (lower Aiguilles Rouges), while a very wide area was accreted in frontal parts within the cover (NAFB and Jura mountains).

In the Aar massif, a similar sequence was described [*Burkhard*, 1988] (Figure 13c): underplating of basement units during the ECM deformation in Late Oligocene to early Miocene times, underplating of basement units and accretion in the cover during the shortening of the upper Gaastern unit, and basement underplating with much larger amount of cover accretion (Jura) during the emplacement of the lower Gaastern unit.

To summarize, underplating is a long-lived process in the north and is characterized locally by high crustal shortening (up to around 60%, considering the basement only, Table 1 and Figures 11, 13b, and 13c). On the contrary, frontal accretion is an important process in the south along with lower crustal shortening (as low as

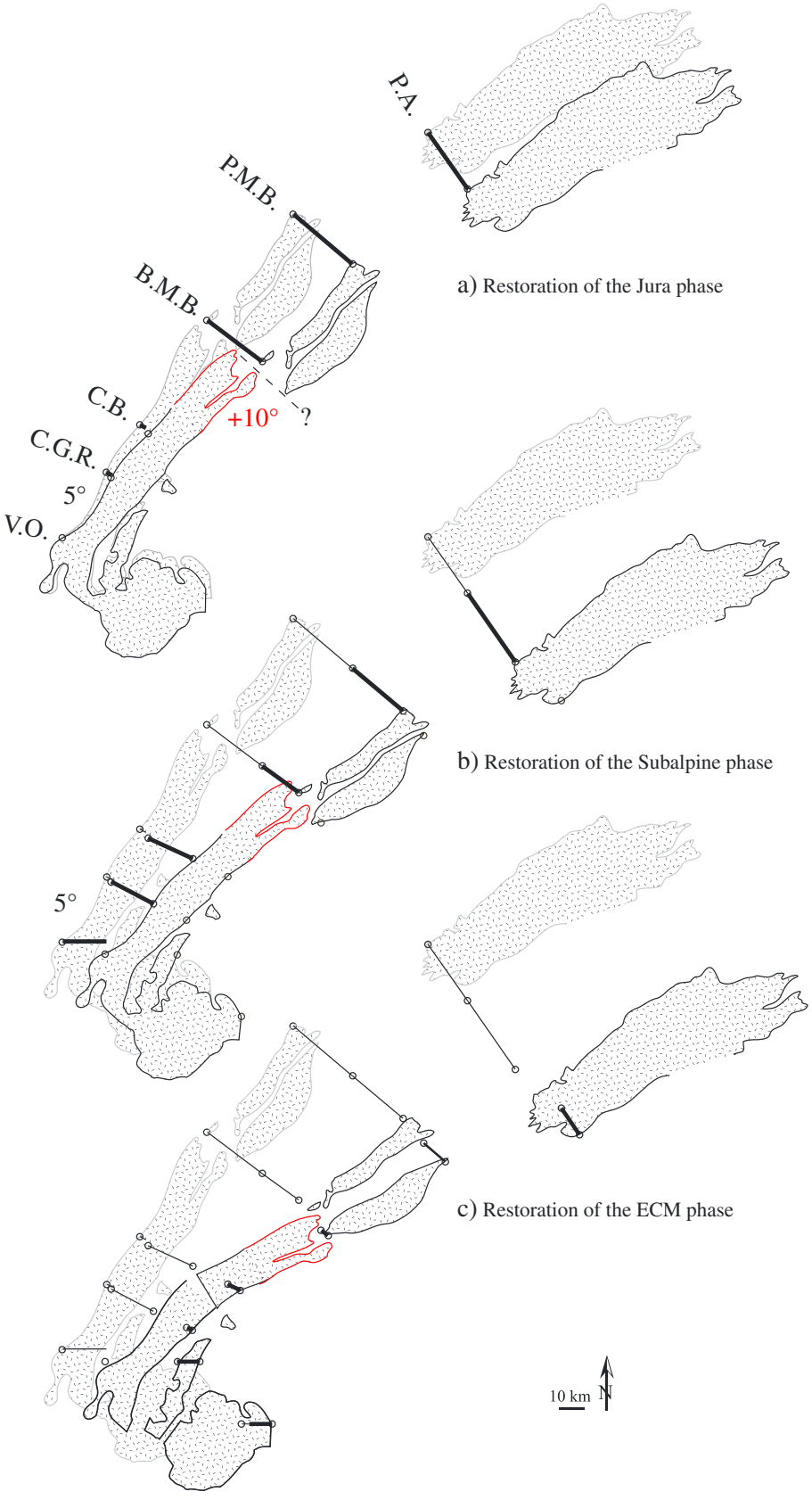

Figure 15

about 25%, Table 1). It is also noteworthy that underplating occurred in the south (ECM shortening), but it is quite different from that in the north, as it occurred in a distributed way (Figure 13a).

This shortening sequence being well defined, we present average long-term rates of shortening (km Ma^{-1}, Figure 14) and exhumation (km Ma^{-1}, Figure 14). We calculated the rate of crustal shortening for each of the defined periods of crustal shortening ("ECM," "Subalpine," and "Jura"). Rates of exhumation are derived from estimated pressure peak (assuming an average density of 2.7 kg/m^3). Available thermochronological data (AFT, ZFT, and UTh/He) are used to derive complementary constraints on exhumation at intermediate depth assuming a steady geotherm of 30°C/km.

The burial rate is estimated using the age of the deepwater turbidites deposition (flysch basin, at the surface) and the age of the pressure peak. It is similar from north to south, about 3 km Ma^{-1} (Figure 14). During the ECM shortening phase, the shortening rate is about 0.8 km Ma^{-1} (11.5 km during 14 Ma, Oligocene times) in the Oisans (Figure 14b), about 1.1 km Ma^{-1} (10.6 km during 10 Ma, Oligocene to early Miocene times) in the Mont Blanc, and about 1.7 km Ma^{-1} (12 km during 7 Ma, early Miocene times) in the Aar.

During the subalpine phase, the shortening rate is about 2.0 km Ma^{-1} (16.5 km during 8 Ma, Miocene times) in the Oisans (Figure 14b), about 3.7 km Ma^{-1} (26 km during 7 Ma, Miocene times) in the Mont Blanc, and about 4.4 km Ma^{-1} (31 km during 7 Ma, early Miocene times) in the Aar (Figure 14a).

During the Jura phase, the shortening rate is about 3.6 km Ma^{-1} (29 km during 8 Ma, late Miocene early Pliocene times) in the Mont Blanc and about 3.2 km Ma^{-1} (26 km during 8 Ma, late Miocene early Pliocene times) in the Aar (Figure 14a).

The crustal shortening rates along the Prealpes-Aar and Prealpes-Mont Blanc sections are about 2 to 3 times higher than along the Vercors-Oisans section, during both the ECM and the subalpine phases. The exhumation rates averaged over these two phases show a rather constant value through time, about 0.2–0.3 km Ma^{-1} for the Oisans massif (Figure 14b), which is consistent with the cooling rates of *Crouzet et al.* [2001]. For the Mont Blanc and the Aar massifs, it is of about 0.8–0.9 km Ma^{-1} (Figure 14a), which is consistent with rates given in *Rolland et al.* [2009] from $^{40}Ar/^{39}Ar$ compared to K-Ar ages [*Kralik et al.*, 1992] for the Aar massif. This is also consistent with fission track dating [*Vernon et al.*, 2008, and references therein]. Similar rates are described for the Mont Blanc over the last 16 Ma [*Seward and Mancktelow*, 1994; *Rolland et al.*, 2008].

Thus, the exhumation rates are also about 3 times higher in the Aar massif than in the Oisans massif. An explanation has to be found for the northward along-strike increase of both the shortening and exhumation rates and will be discussed in the next sections. In any case, the link between the two rates can be explained as follows: (1) assuming shortening rates 3 times higher in the north than in the south and (2) given that the southern massifs are much wider than in the north, it is consistent to find higher exhumation

Figure 15. Displacement field for ECM through time and constraints for palinspastic reconstructions from the shortening sequence; see Table 1 and Figures 3–7. (a) Displacement field of ECM for the Jura phase. The Aar and the Mont Blanc massifs present large displacement, as well as the small basement outcrop between the Belledonne and the Aiguilles Rouges massifs. On the contrary, very few displacements are recorded along the other cross sections. Thus, the displacement field is highly discontinuous. Either there is a large transfer fault between the Belledonne massif and the Aiguilles Rouges-Mont Blanc massifs, or the northern Belledonne massif suffered clockwise rotation. We have arbitrarily rotated back the northern Belledonne massif (in red) of about 10° clockwise. However, this may be less or much more. In any case, a rotation (5° clockwise) is recorded between the Vercors-Oisans and the Chartreuse-Belledonne sections, as the shortening corresponding to the Jura phase is about 2 km for the Chartreuse-Grandes Rousses and the Chartreuse-Belledonne sections. Note that along the Chartreuse-Belledonne section, a shortening slightly higher than 2 km has been taken into account, as a shortening of 2 km would have implied much internal deformation in the ECM. (b) Displacement field of ECM for the subalpine phase. The displacement increases from south to north and witnesses a clockwise rotation of the ECM at the Alpine arc scale. At the massif scale, the south Belledonne massif suffered a clockwise rotation of about 5°. (c) Displacement field during the ECM shortening phase. During this phase, the shortening consists of internal deformation of the ECM. Thus, we cannot simply rigidly move them. However, as their extent represented on the map is their present-day outcrop, we decided not to change their size. We rather decided to assign to the eastern border of each massif the shortening recorded in this massif. Thus, at this step, the "external circle" (west of the thick line) represents the position of a point along the internal border of the ECM, and the "internal circle" (east of the thick line) represents its position before the ECM shortening.

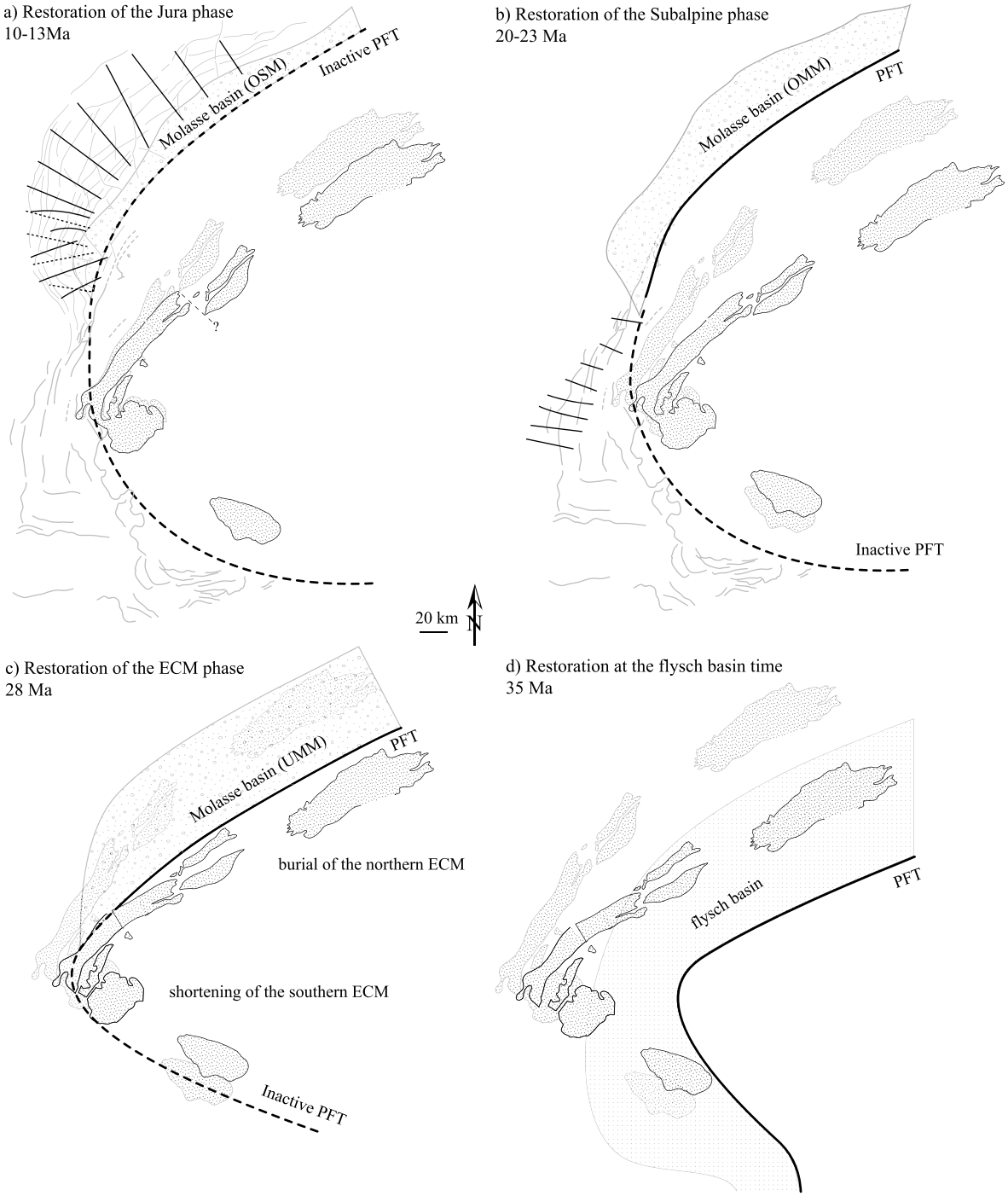

Figure 16. Palinspastic reconstructions at different times. The position of the ECMs derives from the restoration presented in Figure 15 based on the cross sections (Figures 3–7). The position of the basins is from *Ford et al.* [2006] and the cross sections presented in this contribution. (a) Restoration at 10–13 Ma, before the Jura phase. The PFT was inactive during this phase; freshwater clastics deposited (OSM). The straight lines represent the maximum compressive stress in the Jura belt and the dashed lines a late orientation [*Homberg et al.*, 1999]: where only straight lines are represented, the orientation did not change through time. (b) Restoration at around 20 Ma, before the subalpine phase. The northern PFT has been inactive since around 20–25 Ma (onset of the ECM shortening), while the southern part was inactive earlier. Shallow marine clastics deposited (OMM) in the NAFB. The straight lines indicate the maximum compressive stress [*Philippe et al.*, 1998]. (c) Restoration at around 28 Ma. The southern ECMs were already shortening; the southern part of the PFT was inactive. The area where the PFT switched from active to inactive is probably around the same area where the NAFB shallow marine to freshwater clastics laterally end. In the north, the PFT (and the southern limit of the shallow marine to freshwater clastic basin) was located north of the Aiguilles Rouges and Aar massifs as there are no clastics on their cover. (d) Restoration at around 35 Ma, before the shortening of the external zone and during the deepwater turbidites deposition. The northern limit of the turbiditic basin is located north of the Aiguilles Rouges and Aar massifs as their cover presents deepwater turbidite formation. On the contrary, the western limit of the tubiditic basin was probably located east of the Belledonne and Grandes Rousses massifs as no turbidites crops out.

rates in the north. In other words, the exhumation is much more localized in space in the north than in the south.

The Oligo-Miocene collisional kinematics thus varies from south to north along the Alpine arc. Does this along-strike variation of shortening kinematics explain the along-strike variation of the molassic foreland basin dynamics? This basin is well developed, large, and thick in the north (NAFB), while it is very restricted in the south (west of the Oisans) to localized basins [e.g., *Ford and Lickorish*, 2004]. This may be explained by the distributed shortening in the Oisans-Grandes Rousses-Belledonne massifs that almost doubled the orogen width. Such a large orogenic wedge may have prevented the formation of a thick molassic basin.

The localized exhumation of the ECM in the north also explains the preservation of the Préalpes klippen, while no traces of internal units are found in the south as a consequence of the distributed and rather uniform uplift of the ECM and associated erosion of the internal units.

4.4. Palinspastic Tertiary Restorations

The sequence of shortening described above provides a unique opportunity to produce precise palinspastic maps of the Western Alps at different times. Figure 15 shows the way the amount of shortening has been restored for each phase: before the Jura shortening phase (middle to late Miocene, Figure 16a), before the subalpine phase (early Miocene, Figure 16b), before or during the ECM shortening phase (Oligocene, Figure 16c), and during the flysch deposition (Late Eocene, Figure 16d), which is the precollisional stage.

For each step, the position of the ECM is restored according to the sequence and amount of shortening calculated from the cross sections. The sections have been drawn parallel to the local Alpine shortening direction [*Malavieille et al.*, 1984]: E-W for the Oisans massif [*Bellanger et al.*, 2014], and NW-SE for the northern Belledonne massif [*Marquer et al.*, 2006], the Mont Blanc massif [*Gourlay*, 1986; *Leloup et al.*, 2005], and the Aar massif [*Ramsay and Huber*, 1989]. Thus, the restoration can be performed parallel to the section. For the southern section only, the shortening in the subalpine chain (WNW-ESE [*Philippe et al.*, 1998]) is slightly oblique to the section (E-W). This has been taken into account for the palinspastic restoration (Figure 15b).

Figure 16a is the restoration before the Jura shortening phase, at about 10–15 Ma. On this map, one can observe displacement fields and the position of the ECM that vary quite strongly along strike. Indeed, the Jura shortening is strongly not cylindrical at the Alpine arc scale. This phase did not affect the crust at the Oisans latitude; it is responsible for several kilometers of amount of shortening along the Chartreuse-Grandes Rousses (CGR) and Chartreuse-Belledonne (CB) sections (Figure 15a, which implies a rotation of about 5° clockwise of the SW Belledonne massif,) while there is a large shortening along the Préalpes-Mont Blanc (PMB) and the Préalpes-Aar (PA) sections. Similar variations where already noticed by *Affolter et al.* [2008]. On our map, it is noteworthy that a strong variation most likely occurs between the Bornes-Mont Blanc and the Chartreuse-Belledonne sections. Thus, we arbitrarily affected the northern Belledonne massif of a 10° clockwise rotation (Figure 15a) that adds to the rotation induced by the increase of Jura shortening from the Vercors-Oisans section to the Chartreuse-Belledonne one. If no large rotation occurred as suggested in *Heller et al.* [1989], a transfer fault might have been active between the Belledonne and the Mont Blanc massifs (Figure 15a), which is not described in the literature. The (future) thrusts of the Jura belt are represented in Figure 16a, as well as the trend of the maximum compressive principal stress from *Homberg et al.* [1999]. One may observe that the early stress field strongly correlates with our displacement field: the along-strike change of the early compression orientation recorded in the Jura (from NW-SE in the central part to WSW-ENE in the southern part, straight lines, Figure 16a) fits well the shift in our displacement field. Thus, the Aiguilles Rouges and Mont Blanc massifs may have played the role of indenter for the Jura belt. At this time, the Penninic Frontal Thrust (PFT) is inactive as a thrust as all ECM have already started to exhume.

Figure 16b is the restoration before the subalpine phase, at about 20 Ma. The ECMs are restored taking into account the shortening accommodated by the frontal ramps and the subalpine belt. As this shortening increases northward less drastically than for the Jura phase, the displacement pattern shows a more regular rotation with a pole located SW of the Oisans massif (Figure 16b). As a result of this shortening phase, the subalpine belt is activated with the compression trend reported in Figure 16b from *Philippe et al.* [1998]. The PFT became inactive at about 20–25 Ma in the north due to the shortening and exhumation of the ECM [*Leloup et al.*, 2005; *Rolland et al.*, 2008, 2009; *Challandes et al.*, 2008], while it was probably already inactive at

this time in the south as the ECM exhumation started at least at 27 Ma [*van der Beek et al.*, 2010]. It is noteworthy that this sequence of deformation correlates well with the fact that the molassic basin is much more developed in the north [e.g., *Sinclair*, 1997; *Ford et al.*, 2006, and references therein].

Figure 16c is the restoration at 28 Ma. In the south, only part of the shortening of the ECMs has been restored as some shortening has occurred earlier in the Oisans massif [*Simon-Labric et al.*, 2009]. A clockwise rotation of the northern part of the Belledonne massif is implied by our data, especially the shortening along the Chartreuse-Belledonne section. The PFT is most likely active everywhere but gets inactive in the south at about this time (see above).

Figure 16d is the restoration at 35 Ma during the deepwater turbidites deposition. The position of the PFT is quite uncertain but might have been located south of the Aar massif and east of the Oisans massif. It controls the deposition of a large turbiditic flysch-type basin all around the Alpine arc.

During the whole period considered above (from late Eocene to Pliocene), the movement along the PFT also accommodated convergence: from about 110 km in the south to about 200 km in the north (Figure 16). These values added to the shortening estimates from the cross sections (Table 1) provide the following convergence values since 35 Ma for the external zone: around 270 km of convergence for the northern part of the studied area (Mont Bland and Aar massifs) and around 140 km for the southern part (Oisans massif). This variation in convergence along strike the Alpine arc witnesses the rotation of Adria relatively to Europe [*Ustaszewski et al.*, 2008; *Handy et al.*, 2010, and references therein], which is recorded in many ECMs [e.g., *Rolland et al.*, 2008, 2009, 2012]. This rotation may be due to the push of the African plate coupled to the slab rollbacks (especially in western Mediterranean [e.g., *Dewey et al.*, 1989; *Jolivet and Faccenna*, 2000; *Faccenna et al.*, 2004]). Now the questions are as follows: what is the structure of the European margins inherited from Mesozoic times and whether or not they might play a role in the Adria Tertiary rotation?

4.5. Restored Mesozoic Margins

Our reconstruction at 35 Ma provides constraints on the geometry of the European margin in the external zone as no significant collisional deformation occurred before this age, at least north of the Oisans massif where no Pyrenean shortening is described. We assume that a complete crustal breakup occurred in the Valais domain in Western Alps at least around and northeast of the Petit Saint Bernard pass [*Loprieno et al.*, 2010; *Beltrando et al.*, 2012]. There, mantle exhumation occurred with no significant mafic magmatism [*Beltrando et al.*, 2007; *Masson et al.*, 2008]. Thus, there was probably no oceanic crust, although it is still proposed by many authors [see *Handy et al.*, 2010, and references therein].

Moreover, there is no evidence for oceanic spreading west of the Briançonnais domain from the Pyrenees to the Western Alps; there is no metamorphic unit attesting for oceanic subduction, except for the Ligurian one: there is no evidence of HP/LT metamorphism of the Dauphinois margin that would have been due to significant slab pull of an ocean between the Dauphinois and the Briançonnais.

In the Pyrenees, a rifting event is recorded during Albo-Cenomanian times. In southeast France [*Homberg et al.*, 2013, and references therein], a polyphase extensional event is recorded between upper Tithonian and Aptian times. This duration fits particularly well the timing of the Valaisan rifting, if it is Early Cretaceous in age [*Schwizer*, 1984; *Steinmann*, 1994; in *Handy et al.*, 2010; see also *Loprieno et al.*, 2010] but significantly postdates the middle Jurassic Valais rifting according to *Manatschal et al.* [2006], *Mohn et al.* [2010], and *Beltrando et al.* [2012].

Thus, the Pyrenees and southeast France basins may be considered as the rifted transition zone between the Bay of Biscay and the Valais domain. (1) During the Liassic and Dogger times, the Ligurian rifting occurred [*Lemoine et al.*, 1986] as well as possibly the Valais rifting [*Manatschal et al.*, 2006]. (2) The Ligurian ocean started to open during upper Jurassic times. Meanwhile, continental extension continued in southeast France basin [*Homberg et al.*, 2013], possibly in the future Bay of Biscay [*Jammes et al.*, 2009], in the internal Alps (e.g., in the Ligurian Brianconnais [*Bertok et al.*, 2011]), and in the future external Alps: indeed several normal faults active during the upper Jurassic (Figures 3 and 4). The direction of extension may have been similar to the one prevailing during the Ligurian rifting in a strict sense (NW-SE [e.g., *Homberg et al.*, 2013]). (3) During the early Cretaceous, rifting continued in southeast France [*Homberg et al.*, 2013, and references therein] and Pyrenees [*Jammes et al.*, 2009, and references therein] with a possibly N-S direction of extension. Spreading occurred in the Bay of Biscay [Aptian, e.g., *Sibuet et al.*, 2004] and possibly in the east (Aptian times [*Handy et al.*,

2010, and references therein]). The mantle was exhumed during hyperextension during Albo-Cenomanian times in the Pyrenees [e.g., *Jammes et al.*, 2009] and possibly during early Cretaceous in the Valais domain [*Loprieno et al.*, 2010]. In the internal Alps, active normal faults are also reported (external Briançonnais [*Bertok et al.*, 2012]), and in the external Alps, early Cretaceous faults are clearly observed and reported in cross sections (Figures 4 and 7): In the Chartreuse-Grandes Rousses section (Figure 4), *Deville et al.* [1994] showed a strong variation in Mesozoic layer thickness (especially Cretaceous). In the Mont Blanc section (Figure 7), the Chamonix inherited normal fault controlled both Jurassic and Cretaceous depocenters [*Burkhard and Sommaruga*, 1998]. In the Vercors-Oisans section (Figure 3), there might have been a Cretaceous basin in the Grenoble basin, although the complete Mesozoic section lacks above the Belledonne massif. Some of these faults, as well as all the other Mesozoic faults, have similar orientation (NE-SW) as other Mesozoic faults, such as the Cevennes fault system, and were most likely reactivated structures inherited from Variscan times.

In any case, and whatever the age of the Valais domain (middle to late Jurassic or/and early Cretaceous), there must be a transition between an eastern Valais domain with oceanic crust and/or only exhumed mantle and a western rifted domain in southeast France. In other words, one may find a place, between Western and Central Eastern Alps, where the margin evolved through space from hyperextended margin (with mantle exhumation) and/or oceanized domain to a rifted domain with thinned continental crust [e.g., *Mohn et al.*, 2010]. Such setting has been represented in Figure 17. In the following, we discuss the inversion of such margins and their possible effect on the collision kinematics.

First, it is most likely that the increase in amount of (collisional) shortening and total convergence from south to north is not counterbalanced by a northward decrease of (collisional) shortening in the internal units. Such shortening is very difficult to constrain due to the lack of clear passive markers. However, the examination of the geological maps does not suggest that the shortening in the southern internal units is 2 or 3 times greater than in the northern ones. This is consistent with the fact that in the north, the shortening started later than in the south (22 Ma in the Aar Massif [*Rolland et al.*, 2009], 30 Ma in the Mont Blanc massif [*Cenki-Tok et al.*, 2013], and 31–34 Ma in the Oisans massif [*Simon-Labric et al.*, 2009]): the Mesozoic basins between the external Dauphinois and the Briançonnais may have been wider in the north than in the south.

The northward increase of the amount of convergence (including shortening) may thus have been controlled by the basin size and the plate kinematics. Indeed, it is suggested that the Adria motion relative to stable Europe turned from N-S to NW-SE [*Schmid et al.*, 1996] or from NW-SE to almost E-W [*Capitanio and Goes*, 2006] at around 35 Ma or slightly later [see also *Dumont et al.*, 2011, 2012, and references therein]. Given these uncertainties, it is uneasy to discuss the effect of convergence obliquity on along-strike shortening gradient, although it might have an effect. However, such control cannot explain the shortening style differences: indeed the distribution of shortening and exhumation strongly vary from north to south. We here propose that it is, at least in part, controlled by the inherited margin structure.

The southern (Oisans) part of the European margin collided during early Oligocene times. The crust was not buried to more than 10 km depth, and the shortening started along with a coeval or slightly later exhumation. The northern (Mont Blanc, Aar) part of the margin started to shorten (slightly) later but also after a burial twice as large as in the south. This had several consequences that we detail in the next paragraph. But first, we suggest that this may be a direct consequence of the margin structure: in the south, no mantle exhumation occurred between the buoyant Dauphinois and the Briançonnais. Thus, in the absence of negative buoyancy due to oceanic lithosphere or distal hyperextended margin (with no or little crust left), the Dauphinois margin did not subduct significantly and collisional shortening occurred fast after burial, which slowed down the convergence even more. In the north, where the transition between aborted rift and oceanic basin took place (maybe in Central Alps, western Switzerland), the slab pull may have been more important, driving the margin further down, at about 20 km depth. In agreement with increased subduction/underthrusting, a deeper burial in the north may also reflect initially higher crustal strength of the foreland basement, e.g., due to mineralic composition or variable thermotectonic preorogenic history (see *Mouthereau et al.* [2013] for a general discussion).

Such different burial had several consequences. The pressure peak of collisional deformations in Central Alps is about 5 kb. At corresponding depth (20 km), the crust, which may have been originally stronger than southward becomes very weak and ductile during underthrusting (Figure 11d). As a consequence, the basement deformation did not propagate very "fast"/far toward the external area, but deformation in the cover did. A stack of underplated units emplaced leading to an antiformal stack geometry. The exhumation

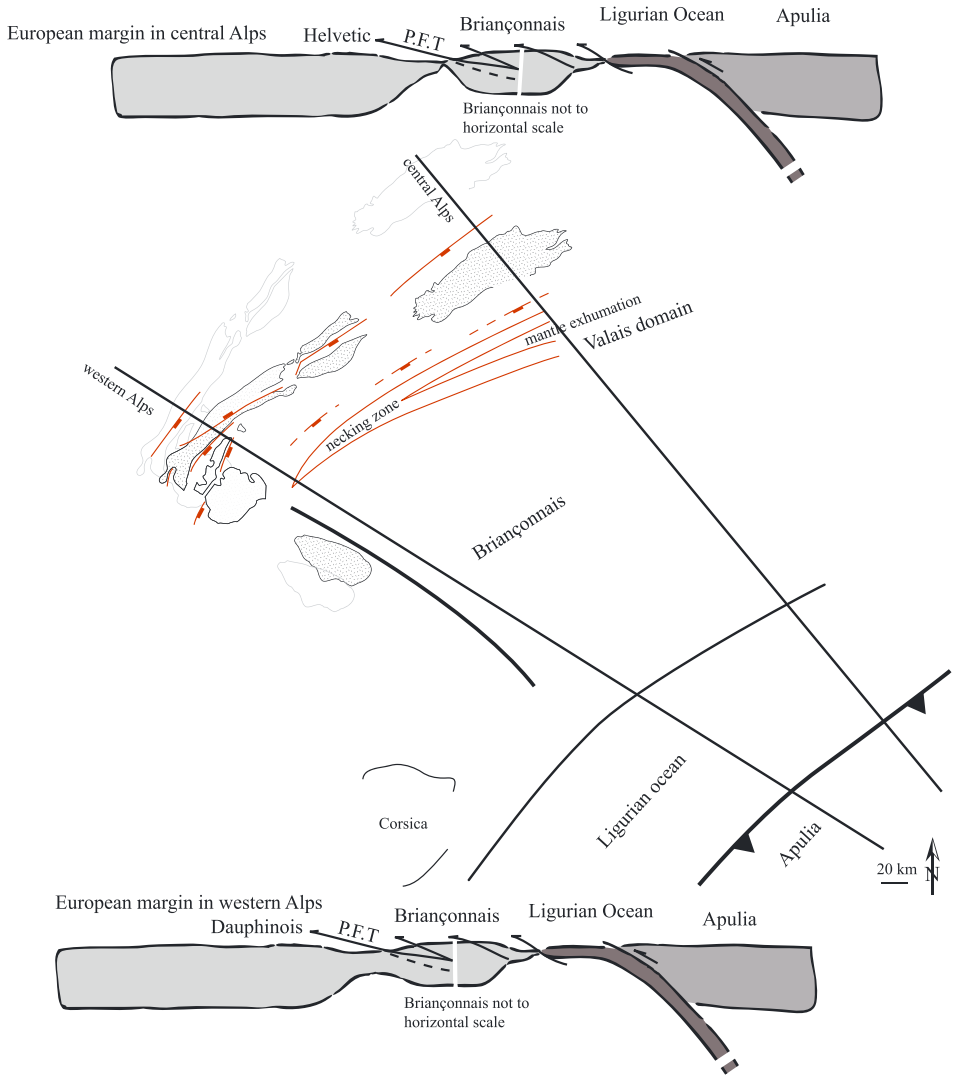

Figure 17. European margin geometry at Mesozoic times (upper Cretaceous). On the palinspastic map. The ECMs are represented in their present-day position (in gray) and in their Cretaceous position (in black). The Mesozoic normal faults have been drawn according to their restored position. The Valais domain terminated westward with a possible large domain in the east (with exhumed mantle?) and a smaller one in the west (rifted domain). Two simplified crustal cross sections of the future Central Alps and Western Alps are presented. The eastern Helvetic domain is much more thinned than the eastern Dauphinois domain.

occurred in a narrow zone, which explains the high exhumation rates. To the south, in Western Alps, the crust burial is about 10 km (Figure 11c), and therefore the crust remained at the brittle-ductile transition. With respect to the north, the basement hence appears relatively stronger. Overall, the thick-skinned deformation dominates and deformation propagates by frontal accretion of basement units; as a consequence, the exhumation is more distributed. We show that the tectonic burial played a key role in modifying the initial crustal rheology. This study complements earlier inferences from global analysis of shortening in thrust belts [*Mouthereau et al.*, 2013] and from numerical modeling [e.g., *Jammes and Huismans*, 2012] showing that in the absence of any tectonic burial an inherently weak crust like the European crust rather implies a distribution of the deformation and a large orogenic wedge.

5. Conclusions

Five balanced cross sections of the whole external zone of the Western Alps provide constraints on the space and time variations of both the amount and the sequence of shortening. Three phases and five units are recognized and are consistent at the scale of the external Western Alps. (1) The "ECM phase" is characterized

by Oligo-Miocene distributed shortening of the ECMs (from Oisans to Aar massifs) and their disharmonically folded cover. Only two tectonic units are detached from their basement: the ultra-Helvetic/Dauphinois units that are present from NE Oisans to around the Aar massif and a unit, called "Aravis-Granier" unit, that corresponds to the upper western ECM cover (Belledonne and Aiguilles Rouges). The latter unit does not extend along strike northeast of the Aiguilles Rouges and SW of Belledonne. (2) The "subalpine phase" is characterized by displacement along basement thrust ramps below the ECMs that transfer deformation up section in a décollement in the Dauphinois cover base responsible for the shortening of the subalpine belts (Vercors, Chartreuse, Bauges, and Bornes massifs) during Middle Miocene times. (3) The "Jura phase" is characterized by basement thrusts below the ECMs that activated a décollement NW of the North Alpine Foreland Basin during upper Miocene to lower Pliocene times.

The amount of crustal shortening determined from the cross sections during each of these phases increases from south (Oisans, total amount of shortening: 28 km) to north (Mont Blanc and Aar, total amount of shortening: 65.9 km or more). The corresponding shortening rates are 2 or 3 times higher in the north than in the south. Similarly, the exhumation rates (from thermochronology and thermobarometry data from the literature) are 2 or 3 times higher in the north (Mont Blanc, Aar) than in the south (Oisans). This relationship is due to shortening by underplating and then localized exhumation in the northern ECM. This shortening distribution probably influenced the North Alpine Foreland Basin that laterally decreased in size southward (toward the Oisans area) where the shortening is more distributed.

The variable localization of the shortening in the Alpine external zone can be explained by the along-strike variations of the inherited margin structure. From the Central Alps to Western Alps, the possible westward decrease of the size of the Valais domain, along with a decrease of the amount of thinning of its margins, may have induced the following consequences: toward the north, where the Valais domain was highly thinned, both the large domain width and the negative buoyancy of its lithosphere ensured a deep burial of the Helvetic margin (down to at least 20 km, Aar and Mont Blanc massifs) strongly reducing the initial crustal strength. Toward the south, where the Valais domain ended and was replaced by the Dauphinois aborted rift, the small width of the basin and its buoyant crust inhibited deep burial (to about 10 km) along with less drastic decrease of the initial crustal strength. As a consequence, in the north the crust was underthrusted, promoting crustal weakening, then underplated with more pronounced shortening of the basement. To the south, the basement was less buried. Hence, the deformation follows characteristic structural style of thick-skinned belt characterized by basement frontal accretion, typical young margins.

Acknowledgments
This work was funded by the Syster program 2010–2011 (INSU-CNRS) and the BRGM contract L10 U 044. This work benefited from discussions with L. Labrousse, C. Rosenberg, A. Verlaguet, L. Bayet, and T. Baudin. We thank F. Roure and M. Beltrando for very constructive reviews.

References

Affolter, T., J.-L. Faure, J.-P. Gratier, and B. Colletta (2008), Kinematic models of deformation at the front of the Alps: New data from map-view restoration, *Swiss J. Geosci.*, *101*(2), 289–303, doi:10.1007/s00015-008-1263-3.

Agard, P., P. Monié, L. Jolivet, and B. Goffé (2002), Exhumation of the Schistes Lustrés complex: In situ laser probe $^{40}Ar/^{39}Ar$ constraints and implications for the Western Alps, *J. Metamorph. Geol.*, *20*(6), 599–618, doi:10.1046/j.1525-1314.2002.00391.x.

Arnaud, H. (1975), *Carte Géologique de la France à 1/50 000: Romand sur Isère (feuille 795)*, BRGM, Orléans.

Bauve, V., R. Plateaux, Y. Rolland, G. Sanchez, N. Béthoux, B. Delouis, and R. Darnault (2014), Long-lasting transcurrent tectonics in SW Alps evidenced by Neogene to present-day stress fields, *Tectonophysics*, doi:10.1016/j.tecto.2014.02.006.

Becker, A. (2000), The Jura Mountains—An active foreland fold-and-thrust belt?, *Tectonophysics*, *321*, 381–406.

Bellahsen, N., L. Jolivet, O. Lacombe, M. Bellanger, A. Boutoux, S. Garcia, F. Mouthereau, L. Le Pourhiet, and C. Gumiaux (2012), Mechanisms of margin inversion in the external Western Alps: Implications for crustal rheology, *Tectonophysics*, *560–561*, 62–83, doi:10.1016/j.tecto.2012.06.022.

Bellanger, M., N. Bellahsen, L. Jolivet, T. Baudin, R. Augier, and A. Boutoux (2014), Basement shear zones development and shortening kinematics in the Ecrins Massif, Western Alps: Shortening in the Ecrins Massif, *Tectonics*, *33*, 84–111, doi:10.1002/2013TC003294.

Beltrando, M., D. Rubatto, R. Compagnoni, and G. Lister (2007), Was the Valaisan basin floored by oceanic crust? Evidence of Permian magmatism in the Versoyen Unit (Valaisan domain, NW Alps), *Ofioliti*, *32*(2), 85–99.

Beltrando, M., G. Frasca, R. Compagnoni, and A. Vitale-Brovarone (2012), The Valaisan controversy revisited: Multi-stage folding of a Mesozoic hyper-extended margin in the Petit St. Bernard pass area (Western Alps), *Tectonophysics*, *579*, 17–36, doi:10.1016/j.tecto.2012.02.010.

Bergerat, F., J. L. Mugnier, S. Guellec, C. Truffert, M. Cazes, B. Damotte, and F. Roure (1990), Extensional tectonics and subsidence of the Bresse basin: An interpretation from ECORS data, *Mém. Soc. Géol. France*, *156*, 145–156.

Bertok, C., L. Martire, E. Perotti, A. d' Atri, and F. Piana (2011), Middle-Late Jurassic syndepositional tectonics recorded in the Ligurian Briançonnais succession (Marguareis–Mongioie area, Ligurian Alps, NW Italy), *Swiss J. Geosci.*, *104*(2), 237–255, doi:10.1007/s00015-011-0058-0.

Bertok, C., L. Martire, E. Perotti, A. d'Atri, and F. Piana (2012), Kilometre-scale palaeoescarpments as evidence for Cretaceous synsedimentary tectonics in the External Briançonnais omain (Ligurian Alps, Italy), *Sediment. Geol.*, *251–252*, 58–75.

Bolliger, T., B. Engesser, and M. Weidmann (1993), Première découverte de mammifères pliocènes dans le Jura neuchâtelois, *Eclogae Geol. Helv.*, *86*, 1031–1068.

Bonnet, C., J. Malavieille, and J. Mosar (2007), Interactions between tectonics, erosion, and sedimentation during the recent evolution of the Alpine orogen: Analogue modeling insights, *Tectonics*, *26*, TC6016, doi:10.1029/2006TC002048.

Bousquet, R., B. Goffé, O. Vidal, R. Oberhänsli, and M. Patriat (2002), The tectono-metamorphic history of the Valaisan domain from the Western to the Central Alps: New constraints on the evolution of the Alps, *Geol. Soc. Am. Bull.*, *114*(2), 207–225.
Boutoux, A., N. Bellahsen, O. Lacombe, A. Verlaguet, and F. Mouthereau (2014), Inversion of pre-orogenic extensional basins in the external Western Alps: Structure, microstructures and restoration, *J. Struct. Geol.*, *60*, 13–29, doi:10.1016/j.jsg.2013.12.014.
Burkhard, M. (1988), L'Helvétique de la bordure occidentale du massif de l'Aar (évolution tectonique et métamorphique), *Eclogae Geol. Helv.*, *81*, 63–114.
Burkhard, M., and A. Sommaruga (1998), Evolution of the western Swiss Molasse basin: Structural relations with the Alps and the Jura belt, *Geol. Soc. London Spec. Publ.*, *134*(1), 279–298, doi:10.1144/GSL.SP.1998.134.01.13.
Capitanio, F. A., and S. Goes (2006), Mesozoic spreading kinematics: Consequences for Cenozoic Central and Western Mediterranean subduction, *Geophys. J. Int.*, *165*(3), 804–816, doi:10.1111/j.1365-246X.2006.02892.x.
Carpena, J. (1992), Fission track dating of zircon: Zircons from Mont Blanc granite (French-Italian Alps), *J. Geol.*, *100*, 411–421.
Cenki-Tok, B., J. R. Darling, Y. Rolland, B. Dhuime, and C. D. Storey (2013), Direct dating of mid-crustal shear zones with synkinematic allanite: New in situ U-Th-Pb geochronological approaches applied to the Mont Blanc massif, *Terra Nova*, *26*, 29–37, doi:10.1111/ter.12066.
Ceriani, S., and S. M. Schmid (2004), From N-S collision to WNW-directed post-collisional thrusting and folding: Structural study of the frontal Penninic units in Savoie (Western Alps, France), *Eclogae Geol. Helv.*, *97*, 347–369.
Ceriani, S., B. Fugenschuh, and S. M. Schmid (2001), Multi-stage thrusting at the "Penninic Front" in the Western Alps between Mont Blanc and Pelvoux massifs, *Int. J. Earth Sci.*, *90*, 685–702.
Challandes, N., D. Marquer, and I. M. Villa (2008), P-T-t modelling, fluid circulation, and ^{39}Ar-^{40}Ar and Rb-Sr mica ages in the Aar Massif shear zones (Swiss Alps), *Swiss J. Geosci.*, *101*(2), 269–288, doi:10.1007/s00015-008-1260-6.
Cochran, J. R., and F. Martinez (1988), Evidence from the northern Red Sea on the transition from continental to oceanic rifting, *Tectonophysics*, *153*, 25–53.
Corsini, M., G. Ruffet, and R. Caby (2004), Alpine and late-hercynian geochronological constraints in the Argentera Massif (Western Alps), *Eclogae Geol. Helv.*, *97*(1), 3–15, doi:10.1007/s00015-004-1107-8.
Crespo-Blanc, A., H. Masson, Z. Sharp, M. Cosca, and J. Hunziker (1995), A stable and ^{40}Ar/^{39}Ar isotope study of a major thrust in the Helvetic nappes (Swiss Alps): Evidence for fluid flow and constraints on nappe kinematics, *Geol. Soc. Am. Bull.*, *107*(10), 1129–1144.
Crouzet, C., G. Ménard, and P. Rochette (2001), Cooling history of the Dauphinoise zone (Western Alps, France) deduced from the thermo-paleomagnetic record: Geodynamic implications, *Tectonophysics*, *340*(1), 79–93.
Deville, É., and A. Chauvière (2000), Thrust tectonics at the front of the Western Alps: Constraints provided by the processing of seismic reflection data along the Chambéry transect, *C.R. Acad. Sci.*, *331*(11), 725–732.
Deville, É., A. Mascle, C. Lamiraux, and A. Le Bras (1994), Tectonic styles, reevaluation of plays in southeastern France, *Oil Gas J.*, *31*, 53–58.
Dewey, J. F., M. L. Helman, S. D. Knott, E. Turco, and D. H. W. Hutton (1989), Kinematics of the western Mediterranean, in *Alpine Tectonics*, *Geol. Soc. London Spec. Publ.*, vol. 45, edited by M. P. Coward, D. Dietrich, and R. G. Parker, pp. 265–283.
Doudoux, B., B. M. de Lepinay, and M. Tardy (1982), Une interprétation nouvelle de la structure des massifs subalpins savoyards (Alpes Occidentales): Nappes de charriage Oligocènes et déformations superposées, *C.R. Acad. Sci.*, *295*, 63–68.
Duchene, S., J. Blichert-Toft, B. Luais, P. Télouk, J.-M. Lardeaux, and F. Albarede (1997), The Lu–Hf dating of garnets and the ages of the Alpine high-pressuremetamorphism, *Nature*, *387*, 586–589.
Dumont, T., J. D. Champagnac, C. Crouzet, and P. Rochat (2008), Multistage shortening in the Dauphine zone (French Alps): The record of Alpine collision and implications for pre-Alpine restoration, *Swiss J. Geosci.*, *101*, 89–S110, doi:10.1007/s00015-008-1280-2.
Dumont, T., T. Simon-Labric, C. Authemayou, and T. Heymes (2011), Lateral termination of the north-directed Alpine orogeny and onset of westward escape in the Western Alpine arc: Structural and sedimentary evidence from the external zone, *Tectonics*, *30*, TC5006, doi:10.1029/2010TC002836.
Dumont, T., S. Schwartz, S. Guillot, T. Simon-Labric, P. Tricart, and S. Jourdan (2012), Structural and sedimentary records of the Oligocene revolution in the Western Alpine arc, *J. Geodyn.*, *56*, 18–38.
Epard, J.-L. (1990), La nappe de Morcles au sud-ouest du Mont Blanc, Mém. Géol. Lausanne 3.
Epard, J.-L., and A. Escher (1996), Transition from basement to cover: A geometric model, *J. Struct. Geol.*, *18*(5), 533–548.
Escher, A., H. Masson, and A. Steck (1993), Nappe geometry in the Western Swiss Alps, *J. Struct. Geol.*, *15*(3–5), 501–509.
Faccenna, C., C. Piromallo, A. Crespo-Blanc, L. Jolivet, and F. Rossetti (2004), Lateral slab deformation and the origin of the western Mediterranean arcs, *Tectonics*, *23*, TC1012, doi:10.1029/2002TC001488.
Fillon, C., R. Huismans, and P. van der Beek (2013), Syntectonic sedimentation effects on the growth of fold-and-thrust belts, *Geology*, *41*, 83–86.
Ford, M. (1996), Kinematics and geometry of early Alpine, basement-involved folds, SW Pelvoux massif, SE France, *Eclogae Geol. Helv.*, *89*, 269–295.
Ford, M., and W. H. Lickorish (2004), Foreland basin evolution around the western Alpine Arc, in *Deep-Water Sedimentation in the Alpine Basin of SE France: New Perspectives on the Gres d'Annot and Related Systems*, *Geol. Soc. London Spec. Publ.*, vol. 221, edited by P. Joseph and S. A. Lomas, pp. 39–63.
Ford, M., W. H. Lickorish, and N. J. Kusznir (1999), Tertiary foreland sedimentation in the Southern Subalpine Chains, SE France: A geodynamic appraisal, *Basi Res.*, *11*, 315–336.
Ford, M., S. Duchene, D. Gasquet, and O. Vanderhaeghe (2006), Two-phase orogenic convergence in the external and internal SW Alps, *J. Geol. Soc. London*, *163*, 815–826, doi:10.1144/0016-76492005-034.
Fry, N. (1989), Southwestward thrusting and tectonics of the Western Alps, *Geol. Soc. London Spec. Publ.*, *45*, 83–109.
Gourlay, P. (1986), La déformation du socle et des couvertures delphino-helvétiques dans la région du Mont-Blanc (Alpes occidentales), *Bull. Soc. Géol. Fr.*, *2*, 159–169.
Guellec, S., J.-L. Mugnier, M. Tardy, and F. Roure (1990), Neogene evolution of the western Alpine foreland in the light of ECORS data and balanced cross-section, *Mém. Soc. Géol. Fr.*, *156*, 165–184.
Handy, M. R., S. M. Schmid, R. Bousquet, E. Kissling, and D. Bernoulli (2010), Reconciling plate-tectonic reconstructions of Alpine Tethys with the geological–geophysical record of spreading and subduction in the Alps, *Earth Sci. Rev.*, *102*(3–4), 121–158, doi:10.1016/j.earscirev.2010.06.002.
Heim, A. (1921), *Geologie der Schweiz*, vol. 2/1, pp. 259–476, Tauchnitz, Leipzig.
Heller, F., W. Lowrie, and A. M. Hirt (1989), A review of palaeomagnetic and magnetic anisotropy results from the Alps, *Geol. Soc. London Spec. Publ.*, *45*(1), 399–420, doi:10.1144/GSL.SP.1989.045.01.22.
Hofmann, B. A., M. Helfer, L. W. Diamond, I. M. Villa, R. Frei, and J. Eikenberg (2004), Topography-driven hydrothermal breccia mineralization of Pliocene age at Grimsel Pass, Aar massif, Central Swiss Alps, *Schweiz. Mineral. Petrogr. Mitt.*, *84*(3), 271–302.
Homberg, C., O. Lacombe, J. Angelier, and F. Bergerat (1999), New constraints for indentation mechanisms in arcuate belts from the Jura Mountains, France, *Geology*, *27*(9), 827–830.

Homberg, C., Y. Schnyder, and M. Benzaggagh (2013), Late Jurassic-Early Cretaceous faulting in the Southeastern French basin: Does it reflect a tectonic reorganization?, *Bull. Soc. Geol. Fr.*, *184*, 501–514.
Huon, S., M. Burkhard, and J.-C. Hunziker (1994), Mineralogical, K-Ar, stable and Sr isotope systematics of K-white micas during very low-grade metamorphism of limestones (Helvetic nappes, western Switzerland), *Chem. Geol.*, *113*(3), 347–376.
Jammes, S., and R. S. Huismans (2012), Structural styles of mountain building: Controls of lithospheric rheologic stratification and extensional inheritance, *J. Geophys. Res.*, *117*, B10403, doi:10.1029/2012JB009376.
Jammes, S., G. Manatschal, L. Lavier, and E. Masini (2009), Tectonosedimentary evolution related to extreme crustal thinning ahead of a propagating ocean: Example of the western Pyrenees, *Tectonics*, *28*, TC4012, doi:10.1029/2008TC002406.
Jolivet, L., and C. Faccenna (2000), Mediterranean extension and the Africa-Eurasia collision, *Tectonics*, *19*(6), 1095–1106, doi:10.1029/2000TC900018.
Jullien, M., and B. Goffé (1993), Cookeite and pyrophyllite in the Dauphinois black shales (Isère, France): Implications for the conditions of metamorphism in the Alpine external zones, *Schweiz. Mineral. Petrogr. Mitt.*, *73*, 257–363.
Kalin, D. (1997), Litho-and biostratigraphy of the mid-to late Miocene Bois de Raube-formation (Northwestern Switzerland), *Eclogae Geol. Helv.*, *90*, 97–114.
Kempf, O., and O. A. Pfiffner (2004), Early Tertiary evolution of the North Alpine Foreland Basin of the Swiss Alps and adjoining areas, *Basin Res.*, *16*(4), 549–567, doi:10.1111/j.1365-2117.2004.00246.x.
Kerckhove, C. (1969), La "zone du Flysch" dans les nappes de l'Embrunais-Ubaye (Alpes occidentales), *Géol. Alp.*, *45*, 5–204.
Kirschner, D. L., M. A. Cosca, H. Masson, and J. C. Hunziker (1996), Staircase 40/Ar39Ar spectra of fine-grained white mica: Timing and duration of deformation and empirical constraints on argon diffusion, *Geology*, *24*(8), 747–750.
Kralik, M., N. Clauer, R. Holnsteiner, H. Huemer, and F. Kappel (1992), Recurrent fault activity in the Grimsel Test Site (GTS, Switzerland): Revealed by Rb-Sr, K-Ar and tritium isotope techniques, *J. Geol. Soc.*, *149*(2), 293–301, doi:10.1144/gsjgs.149.2.0293.
Lacombe, O., and F. Mouthereau (2002), Basement-involved shortening and deep detachment tectonics in forelands of orogens: Insights from recent collision belts (Taiwan, Western Alps, Pyrénées), *Tectonics*, *21*(4), 1030, 10.1029/2001TC901018.
Leloup, P., N. Arnaud, E. Sobel, and R. Lacassin (2005), Alpine thermal and structural evolution of the highest external crystalline massif: The Mont Blanc, *Tectonics*, *24*, TC4002, doi:10.1029/2004TC001676.
Lemoine, M., et al. (1986), The continental margin of the Mesozoic Tethys in the Western Alps, *Mar. Pet. Geol.*, *3*, 179–199.
Loprieno, A., R. Bousquet, S. Bucher, S. Ceriani, F. H. Dalla Torre, B. Fügenschuh, and S. M. Schmid (2010), The Valais units in Savoy (France): A key area for understanding the palaeogeography and the tectonic evolution of the Western Alps, *Int. J. Earth Sci.*, *100*(5), 963–992, doi:10.1007/s00531-010-0595-1.
Malavieille, J., R. Lacassin, and M. Mattauer (1984), Signification tectonique des linéations d'allongement dans les Alpes occidentales, *Bull. Soc. Géol. Fr.*, *26*(5), 895–906.
Manatschal, G., A. Engström, L. Desmurs, U. Schaltegger, M. Cosca, O. Müntener, and D. Bernoulli (2006), What is the tectono-metamorphic evolution of continental break-up: The example of the Tasna Ocean–Continent Transition, *J. Struct. Geol.*, *28*(10), 1849–1869, doi:10.1016/j.jsg.2006.07.014.
Marquer, D. (1990), Structure et déformation alpine dans les granites hercyniens du massif du Gothard (Alpes centrales suisses), *Eclogae Geol. Helv.*, *83*, 77–97.
Marquer, D., P. Calcagno, J. C. Barfety, and T. Baudin (2006), 3D modeling and kinematics of the external zone of the French Western Alps (Belleclonne and Grand Chatelard Massifs, Maurienne Valley, Savoie), *Eclogae Geol. Helv.*, *99*, 211–222, doi:10.1007/s00015-006-1183-z.
Masson, H., F. Bussy, M. Eichenberger, N. Giroud, C. Meilhac, and S. Presniakov (2008), Early Carboniferous age of the Versoyen ophiolites and consequences: Non-existence of a "Valais ocean"(Lower Penninic, Western Alps), *Bull. Soc. Géol. Fr.*, *179*(4), 337–355.
Ménard, G., and F. Thouvenot (1987), Coupes équilibrées crustales: Méthodologie et application aux Alpes occidentales, *Geodin. Acta*, *1*, 35–45.
Michalski, I., and M. Soom (1990), The Alpine thermo-tectonic evolution of the Aar and Gotthard massifs, central Switzerland: Fission track ages on zircon and apatite and K-Ar mica ages, *Schweiz. Mineral. Petrogr. Mitt.*, *70*, 373–387.
Mohn, G., G. Manatschal, O. Müntener, M. Beltrando, and E. Masini (2010), Unravelling the interaction between tectonic and sedimentary processes during lithospheric thinning in the Alpine Tethys margins, *Int. J. Earth Sci.*, *99*(S1), 75–101, doi:10.1007/s00531-010-0566-6.
Mouthereau, F., A. B. Watts, and E. Burov (2013), Structure of orogenic belts controlled by lithosphere age, *Nat. Geosci.*, *6*(9), 785–789, doi:10.1038/ngeo1902.
Mugnier, J.-L., S. Guellec, G. Ménard, F. Roure, M. Tardy, and P. Vialon (1990), A crustal scale balanced cross-section through the external Alps deduced from the ECORS profile, *Mém. Soc. Géol. Fr.*, *156*, 203–216.
Mulder, T., et al. (2010), High-resolution analysis of submarine lobes deposits: Seismic-scale outcrops of the Lauzanier area (SE Alps, France), *Sediment. Geol.*, *229*(3), 160–191, doi:10.1016/j.sedgeo.2009.11.005.
Oberhänsli, R., et al. (2004), Map of the metamorphic structure of the Alps (1:1'000'000), Commission for the Geological Map of the World (UNESCO), Paris.
Pfiffner, O. A., S. Sahli, and M. Stauble (1997), Structure and evolution of the external basement massifs (Aar, Aiguilles Rouges/Mt. Blanc), in *Deep Structure of the Swiss Alps: Results from NRP 20*, pp. 139–153, Springer, New York.
Philippe, Y., E. Deville, and A. Mascle (1998), Thin-skinned inversion tectonics at oblique basin margins: Example of the western Vercors and Chartreuse Subalpine massifs (SE France), in *Cenozoic Foreland Basins of Western Europe*, *Geol. Soc. London Spec. Publ.*, vol. 134, edited by A. Mascle et al., pp. 239–262.
Ramsay, J. (1981), Tectonics of the Helvetic nappes, in *Thrust and Nappe Tectonics*, Special Publications, vol. 9, pp. 293–309, Geological Society, London.
Ramsay, J. G., and M. Huber (1989), *Strain Analysis, The Techniques of Modern Structural Geology*, vol. 1, Academic Press, London.
Ramsay, J. G., M. Casey, and R. Kligfield (1983), Role of shear in the developpement of the Helvetic fold-thrust belt of Switzerland, *Geology*, *11*, 439–442.
Reinecker, J., M. Danišík, C. Schmid, C. Glotzbach, M. Rahn, W. Frisch, and C. Spiegel (2008), Tectonic control on the late stage exhumation of the Aar Massif (Switzerland): Constraints from apatite fission track and (U-Th)/He data, *Tectonics*, *27*, TC6009, doi:10.1029/2007TC002247.
Rolland, Y., S. Cox, A.-M. Boullier, G. Pennacchioni, and N. Mancktelow (2003), Rare earth and trace element mobility in mid-crustal shear zones: Insights from the Mont Blanc Massif (Western Alps), *Earth Planet. Sci. Lett.*, *214*(1–2), 203–219, doi:10.1016/S0012-821X(03)00372-8.
Rolland, Y., M. Rossi, S. F. Cox, M. Corsini, N. Mancktelow, G. Pennacchioni, M. Fornari, and A. M. Boullier (2008), $^{40}Ar/^{39}Ar$ dating of synkinematic white mica: Insights from fluid-rock reaction in low-grade shear zones (Mont Blanc Massif) and constraints on timing of deformation in the NW external Alps, *Geol. Soc. London Spec. Publ.*, *299*(1), 293–315, doi:10.1144/SP299.18.
Rolland, Y., S. F. Cox, and M. Corsini (2009), Constraining deformation stages in brittle-ductile shear zones from combined field mapping and Ar-40/Ar-39 dating: The structural evolution of the Grimsel Pass area (Aar Massif, Swiss Alps), *J. Struct. Geol.*, *31*, 1377–1394.
Rolland, Y., J.-M. Lardeaux, and L. Jolivet (2012), Deciphering orogenic evolution, *J. Geodyn.*, *56–57*, 1–6.

Rossi, M., Y. Rolland, O. Vidal, and S. F. Cox (2005), Geochemical variations and element transfer during shear zone development and related episyenites at middle crust depths: Insights from the study of the Mont-Blanc Granite (French-Italian Alps), *Geol. Soc. London Spec. Publ.*, *245*, 373–396.

Rubatto, D., and J. Hermann (2001), Exhumation as fast as subduction?, *Geology*, *29*(1), 3–6.

Sanchez, G., Y. Rolland, J. Schneider, M. Corsini, E. Oliot, P. Goncalves, C. Verati, J.-M. Lardeaux, and D. Marquer (2011), Dating low-temperature deformation by $^{40}Ar/^{39}Ar$ on white mica, insights from the Argentera-Mercantour Massif (SW Alps), *Lithos*, *125*, 521–536.

Schmid, S. M., O. A. Pfiffner, N. Froitzheim, G. Schönborn, and E. Kissling (1996), Geophysical-geological transect and tectonic evolution of the Swiss-Italian Alps, *Tectonics*, *15*, 1036–1064, doi:10.1029/96TC00433.

Schwizer, B. (1984), Die Tristel-Formation. Vergleichende Untersuchungen in Graubünden, Liechtenstein, Vorarlberg und Bayern, PhD Thesis, Univ. of Bern.

Seward, D., and N. S. Mancktelow (1994), Neogene kinematics of the central and Western Alps: Evidence from fission-track dating, *Geology*, *22*(9), 803–806.

Sibuet, J. C., S. P. Srivastava, and W. Spakman (2004), Pyrenean orogeny and plate kinematics, *J. Geophys. Res.*, *109*, doi:10.1029/2003JB002514.

Simon-Labric, T., Y. Rolland, T. Dumont, T. Heymes, C. Authemayou, M. Corsini, and M. Fornari (2009), Ar-40/Ar-39 dating of Penninic Front tectonic displacement (W Alps) during the Lower Oligocene (31–34 Ma), *Terra Nova*, *21*, 127–136.

Sinclair, H. D. (1997), Tectonostratigraphic model for underfilled peripheral foreland basins: An Alpine perspective, *Geol. Soc. Am. Bull.*, *109*, 324–346.

Sinclair, H. D., and P. A. Allen (1992), Vertical versus horizontal motions in the Alpine orogenic wedge: Stratigraphic response in the foreland basin, *Basin Res.*, *4*, 215–232.

Soom, M. A. (1990), Abkuhlungs- und Hebungsgeschichte der Externmassive und der Penninischen decken beidseits der Simplon-Rhone-Linie seit dem Oligozan: Spaltspurdatierungen an apatit/zirkon und K/Ar-datierungen an biotit/muskowit (westliche zentralalpen), PhD, Univ. of Bern.

Stampfli, G. M., G. D. Borel, R. Marchant, and J. Mosar (2002), Western Alps geological constraints on western Tethyan reconstructions, *J. Virtual Explor.*, *8*, 77–106.

Steck, A., J. L. Epard, A. Escher, P. Lehner, R. Marchant, and H. Masson (1997), Geological interpretation of the seismic profiles through western Switzerland: Rawil (W1), Val d'Anniviers (W2), Mattertal (W3), Zmutt-Zermatt-Findelen (W4) and Val de Bagnes (W5), in *Deep Structure of the Swiss Alps: Results from NRP 20*, edited by O. A. Pfiffner et al., pp. 123–138, Birkhäuser Verlag, Basel: Boston.

Steiniger, F. F., W. A. Berggren, D. V. Kent, R. L. Bernor, S. Sen, and J. Agusti (1996), Circum-Mediterranean Neogene (Miocene and Pliocene) marine-continental chronologic correlations of European Mammal Units, in *The Evolution of Western Eurasian Neogene Mammal Faunas*, edited by R. L. Bernor, V. Fahlbusch, and H.-W. Mittmann, pp. 7–46, Columbia Univ. Press, New York.

Steinmann, M. (1994), Ein Beckenmodell für das Nordpenninikum der Ostschweiz, *Jahrb. Geol. Bundesanst.*, *137*, 675–721.

Taylor, B., A. Goodliffe, F. Martinez, and R. Hey (1995), Continental rifting and initial sea-floor spreading in the Woodlark basin, *Nature*, *374*, 534–537.

Trumpy, R. (1975), Penninic-Austroalpine boundary in the Swiss Alps: A presumed former continental margin and its problem, *Am. J. Sci.*, *279*, 209–238.

Ustaszewski, K., S. M. Schmid, B. Fugenschuh, M. Tischler, E. Kissling, and W. Spakman (2008), A map-view restoration of the Alpine–Carpathian–Dinaridic system for the Early Miocene, *Swiss J. Geosci.*, *101*, 273–294, doi:10.1007/s00015-008-1288-7.

Van der Beek, P. A., P. G. Valla, F. Herman, J. Braun, C. Persano, K. J. Dobson, and E. Labrin (2010), Inversion of thermochronological age-elevation profiles to extract independent estimates of denudation and relief history—II: Application to the French Western Alps, *Earth Planet. Sci. Lett.*, *296*, 9–22.

Vernon, A. J., P. A. van der Beek, H. D. Sinclair, and M. K. Rahn (2008), Increase in late Neogene denudation of the European Alps confirmed by analysis of a fission-track thermochronology database, *Earth Planet. Sci. Lett.*, *270*(3–4), 316–329, doi:10.1016/j.epsl.2008.03.053.

Wibberley, C. (1999), Are feldspar-to-mica reactions necessarily reaction-softening processes in fault zones?, *J. Struct. Geol.*, *21*, 1219–1227.

Erratum

In the originally published version of this article, the scale bars for Figures 3-7 were incorrect. The errors have since been corrected and this version may be considered the authoritative version of record.